OPEN ACCESS

TRANSLATIONAL SCIENCE

Auxilin is a novel susceptibility gene for congenital heart block which directly impacts fetal heart function

Sabrina Meisgen,[1] Malin Hedlund,[1] Aurelie Ambrosi,[1] Lasse Folkersen,[1,2] Vijole Ottosson,[1] David Forsberg,[3] Gudny Ella Thorlacius,[1] Luca Biavati,[4] Linn Strandberg,[1] Johannes Mofors,[1] Daniel Ramskold,[1] Sabrina Ruhrmann,[5] Lauro Meneghel,[1] William Nyberg,[1] Alexander Espinosa,[1] Robert Murray Hamilton,[6] Anders Franco-Cereceda,[7] Anders Hamsten,[1] Tomas Olsson,[5] Lois Greene,[8] Per Eriksson,[1] Kristina Gemzell-Danielsson,[3] Stina Salomonsson,[1] Vijay K Kuchroo,[9] Eric Herlenius,[3] Ingrid Kockum,[5] Sven-Erik Sonesson,[3] Marie Wahren-Herlenius [1,10]

Handling editor Josef S Smolen

► Additional supplemental material is published online only. To view, please visit the journal online (http://dx.doi.org/10.1136/annrheumdis-2021-221714).

For numbered affiliations see end of article.

Correspondence to
Professor Marie Wahren-Herlenius, Department of Medicine, Karolinska Institute, Stockholm, Stockholm, Sweden; marie.wahren@ki.se

Received 20 October 2021
Accepted 11 April 2022
Published Online First
25 April 2022

To cite: Meisgen S, Hedlund M, Ambrosi A, *et al*. *Ann Rheum Dis* 2022;**81**:1151–1161.

ABSTRACT

Objective Neonatal lupus erythematosus (NLE) may develop after transplacental transfer of maternal autoantibodies with cardiac manifestations (congenital heart block, CHB) including atrioventricular block, atrial and ventricular arrhythmias, and cardiomyopathies. The association with anti-Ro/SSA antibodies is well established, but a recurrence rate of only 12%–16% despite persisting maternal autoantibodies suggests that additional factors are required for CHB development. Here, we identify fetal genetic variants conferring risk of CHB and elucidate their effects on cardiac function.

Methods A genome-wide association study was performed in families with at least one case of CHB. Gene expression was analysed by microarrays, RNA sequencing and PCR and protein expression by western blot, immunohistochemistry, immunofluorescence and flow cytometry. Calcium regulation and connectivity were analysed in primary cardiomyocytes and cells induced from pleuripotent stem cells. Fetal heart performance was analysed by Doppler/echocardiography.

Results We identified *DNAJC6* as a novel fetal susceptibility gene, with decreased cardiac expression of *DNAJC6* associated with the disease risk genotype. We further demonstrate that fetal cardiomyocytes deficient in auxilin, the protein encoded by *DNAJC6*, have abnormal connectivity and Ca^{2+} homoeostasis in culture, as well as decreased cell surface expression of the $Ca_v1.3$ calcium channel. Doppler echocardiography of auxilin-deficient fetal mice revealed cardiac NLE abnormalities in utero, including abnormal heart rhythm with atrial and ventricular ectopias, as well as a prolonged atrioventricular time intervals.

Conclusions Our study identifies auxilin as the first genetic susceptibility factor in NLE modulating cardiac function, opening new avenues for the development of screening and therapeutic strategies in CHB.

Key messages

What is already known about this subject?

⇒ Congenital heart block may develop after transplacental transfer of maternal autoantibodies.

⇒ A recurrence rate of only 12%–16% despite persisting maternal autoantibodies suggests that additional factors are required for congenital heart block (CHB) development.

What does this study add?

⇒ We here identify fetal genetic variants conferring risk of CHB and elucidate their effects on cardiac function.

How might this impact on clinical practice or future developments?

⇒ The findings open new avenues for the development of screening and therapeutic strategies in CHB.

INTRODUCTION

Neonatal lupus erythematosus (NLE) may develop in children of rheumatic women with autoantibodies to the Ro/SSA and La/SSB antigens.[1–4] The most common manifestations of NLE are skin rash and congenital heart block (CHB). While the former is most often benign and resolves as maternal autoantibodies are cleared from the child's circulation, the latter is characterised by an irreversible disruption of electric signal conduction at the atrioventricular (AV) node (third-degree AV block) and has a high mortality rate around 20% if left untreated,[5] with survivors often requiring pacemaker implants for the remainder of their life.[6 7]

CHB typically develops between weeks 18–24 of pregnancy and is often detected when the fetus presents with signs of bradycardia and complete AV block. The bradycardia is preceded and paralleled by other cardiac pathologies leading up to the end-stage third-degree AV block caused by fibrosis and calcification of the AV node.[8 9] Sinus node dysfunction, lower-degree AV block and a prolonged isovolumetric contraction time have thus been observed in early stages of CHB.[10–12] Up to 15%–20% of fetuses affected by CHB have also been shown to develop more diverse myocardial manifestations before birth,[13 14] and signs of junctional ectopic tachycardia or ventricular tachycardia have been reported in nearly one third of fetuses with CHB.[15 16] CHB thus collectively refers to the spectrum of fetal cardiac manifestations occurring in neonatal lupus.

An association between CHB and the presence of maternal autoantibodies to the Ro/SSA autoantigen has long been established, and, when the diagnosis of fetal third-degree AV block without major malformations is established in utero, more than 95% of the mothers test positive for anti-Ro/SSA antibodies.[17] However, a recurrence rate of only approximately 12%–16% for second/third-degree AV block despite persisting maternal autoantibodies indicates that fetal susceptibility, governed by genetic factors, may contribute to disease development.[18–21] Fetal MHC alleles have been linked to the susceptibility, but no other genes thus far.[22–24] In this study, we, therefore, aimed at identifying genetic variants related to CHB by performing a genome-wide association study in families with at least one case of CHB, and sought to define the biological and functional relevance of identified candidate gene(s) for CHB.

PATIENTS AND METHODS

A detailed Patients and Methods section is available in online supplemental materials.

Study population and genotyping

The cohort of patients diagnosed with CHB (n=92) and their families has been previously described.[17 18] Briefly, AVB II–III in the index case and confirmed maternal Ro/SSA autoantibodies constituted inclusion criteria for a family, and families in which the index case had major cardiac structural abnormalities, postoperative or infection-induced block were excluded. Maternal diagnoses at the time of blood sampling were primary Sjögren's syndrome (n=14), SLE (n=12), SLE with secondary Sjögren's syndrome (n=18), rheumatoid arthritis (n=1), rheumatoid arthritis with secondary Sjögren's syndrome (n=1), while 39 mothers had no rheumatic diagnosis. Information was not available for two mothers. Anti-Ro52 autoantibodies were present in 96% of the mothers, anti-Ro60 in 61% and anti-La antibodies in 58%. Other analysed autoantibodies (anti-Histone, and-SmB, anti-SmD, anti-RNP, anti-Cenp-B and Ribosomal P) were present in less than 10% of the mothers (online supplemental table 1).

Genotyping was performed on the Illumina 660W-Quad Beadchip.

Statistical analysis

Genome-wide associations were analysed using PLINK. Statistica and SigmaPlot were used for analysing Doppler-recorded data. Graphpad Prism V.5 was used for all other statistical tests. The statistical tests used for analysis of data from individual experiments are stated in respective figure legend.

RESULTS

Identification of Auxilin/*DNAJC6* as a susceptibility gene for CHB

To identify genes that influence fetal susceptibility to CHB, we performed a genome-wide association study of >5 00 000 single-nucleotide polymorphisms (SNP) in a population-based cohort of families with children diagnosed with CHB. To segregate CHB-unique disease traits from potential inherited maternal traits reflecting the maternal rheumatic autoimmune status, we used a family-based study strategy and included SNP genotype data from index cases and their parents and unaffected siblings.

Analysing transmission of SNPs based on genotypes of index cases (n=92) and first-degree relatives (n=256) using the family-based association for disease trait (DFAM) method, we identified 32 polymorphisms associated with CHB at $p\leq1\times10^{-4}$ (figure 1A, online supplemental figure 1 and online supplemental table 2). Subsequent validation analysis of these 32 CHB-associated polymorphisms in a population-based case-control (C-C) set-up confirmed the association of the locus on chromosome 1p31.3 at a higher level of significance (rs1570868, $P_{DFAM}=3\times10^{-5}$ and $P_{C\text{-}C}=6\times10^{-6}$), and verified suggestive associations in two other genomic regions 1q24.2 (rs7552323, $P_{DFAM}=3\times10^{-5}$, $P_{C\text{-}C}=2\times10^{-4}$) and 3p25.1 (rs1993331, $P_{DFAM}=5\times10^{-5}$ and $P_{C\text{-}C}=3\times10^{-4}$; rs2730335, $P_{DFAM}=5\times10^{-5}$ and $P_{C\text{-}C}=5\times10^{-4}$; and rs2730367, $P_{DFAM}=5\times10^{-5}$ and $P_{C\text{-}C}=2\times10^{-4}$) (figure 1B and online supplemental table 3). Parental transmission of the risk alleles to the affected individuals was 75% (95% CI 63.6% to 83.8%) for rs1570868, 80% (95% CI 60% to 71%) for rs7552323% and 78% (95% CI 64.4% to 87.3%) for rs1993331, rs2730335, and rs2730367, respectively (figure 1C and online supplemental table 2). ORs for the same SNPs in the validation analysis were 2.01 (95% CI 1.50 to 2.81) for rs1570868, 1.82 (95% CI 1.33 to 2.49) for rs7552323 and ranged between 1.82 and 1.90 (95% CI 1.30 to 2.67) for rs1993331, rs2730335 and rs2730367 (figure 1D and online supplemental table 3). Closer examination of the associated locus on chr 1p31.3 revealed the highest association with intronic variants in *DNAJC6* (figure 1E, online supplemental table 2).

Expression quantitative trait loci (eQTL) analysis in cardiac tissue of the genes present in the regions surrounding the top replicating SNPs (±500 kb) revealed a significant effect of rs1570868 on the expression of the *DNAJC6* gene, but not on the expression of other genes in the chromosomal interval (figure 2A). Interestingly, individuals carrying the risk allele at this position had a lower cardiac *DNAJC6* expression compared with carriers of the non-risk allele (figure 2B). Notably, *DNAJC6* expression in other tested tissues was not affected by the rs1570868 polymorphism (figure 2C and data not depicted).

DNAJC6 encodes the putative tyrosine-protein phosphatase auxilin, which is involved in clathrin-mediated endocytosis. Four protein-coding transcripts have been predicted for auxilin (figure 2D), and we could confirm expression of all four variants in cardiac tissue by qPCR (figure 2E, online supplemental figure 2). Auxilin-201 is the only transcript conserved between human and mouse, suggesting that it may be important functionally. Interestingly, analysis of transcript-specific auxilin expression according to the rs1570868 genotypes revealed that carriers of the CHB risk allele have a lower expression of auxilin-201 compared with carriers of the non-risk allele ($p<7\times10^{-4}$) (figure 2F). In contrast, cardiac expression levels of the three other transcript variants are not affected by the rs1570868 SNP.

Auxilin is highly expressed in the fetal heart and colocalised with clathrin in vesicular structures in primary cardiomyocytes

To address the functional basis for auxilin deficiency involvement in CHB, we first investigated whether auxilin is expressed in the heart during fetal development. We found that auxilin is indeed expressed in human fetal cardiac tissue both before and during the risk period for CHB development (figure 3A and online supplemental figure 3A-C). Interestingly, auxilin expression is remarkably higher in the fetal heart compared with the adult heart (figure 3A), as well as in comparison with other fetal tissues (figure 3B). Of note, cardiac tissue

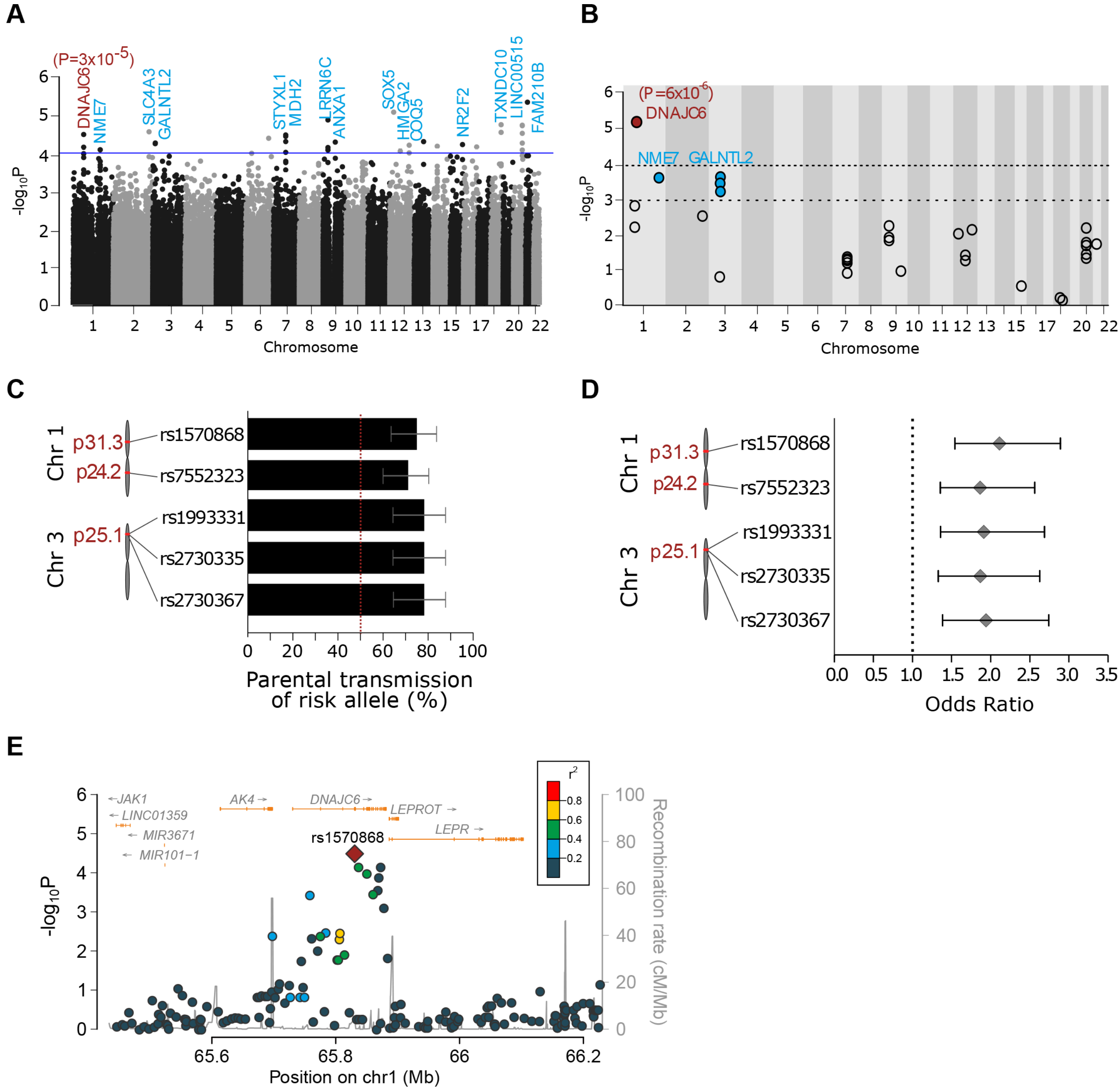

Figure 1 Identification of novel genomic loci associated with CHB. (A) Manhattan plot of genome-wide family-based association for disease trait (DFAM) transmission statistics based on SNP genotyping of CHB cases (n=92) and first-degree relatives (n=256). (B) Logistic regression analysis of association statistics for SNPs with $P_{DFAM} \leq 1\times10^{-4}$ comparing CHB cases (n=89) vs 1195 population-based out-of-study controls. Replicating polymorphisms with $p\leq1\times10^{-4}$ (red) and $p\leq1\times10^{-3}$ (blue). Approximate chromosomal positions are indicated. Dashed lines indicates $p=1\times10^{-4}$ and $p\leq1\times10^{-3}$ (A, B). (C) Percentage of parental transmission to CHB cases (95% CI) for replicating risk variants (DFAM analysis). Dashed line indicates 50% transmission. (D) OR (95% CI) for replicating risk variants (logistic regression). Dashed line indicates OR=1.0. (E) LocusZoom (http://locuszoom.org/) plot of the associated *DNAJC6* region on chromosome 1. CHB, congenital heart block; SNP, single-nucleotide polymorphisms;

expression profiling not only confirmed high expression of auxilin in fetal heart but also revealed that the homologous cyclin-G associated kinase (GAK), also denoted auxilin-2, is expressed only at low levels in the fetal heart (figure 3C). This relation is reversed in adult cardiac tissue, where auxilin is expressed at lower levels than GAK (figure 3D), suggesting that lack of auxilin may specifically affect the fetal rather than the adult heart. Auxilin expression was confirmed at RNA expression level (online supplemental figure 3D-F) and the protein level by immunoblotting of human fetal cardiac tissue and in cardiomyocytes (figure 3E–I). Ubiquitous expression of auxilin was observed throughout the fetal heart by immunohistochemistry (figure 3J), and these data were confirmed by similar auxilin expression levels in human fetal cardiac tissue surgically dissected from the apical myocardium and from the AV node (figure 3K and online supplemental figure 3G-I). Immunofluorescence staining of single cell preparations of human fetal cardiomyocytes demonstrated subcellular localisation of auxilin, which is present in the cytoplasm in a vesicular pattern and partly colocalises with clathrin (figure 3L).

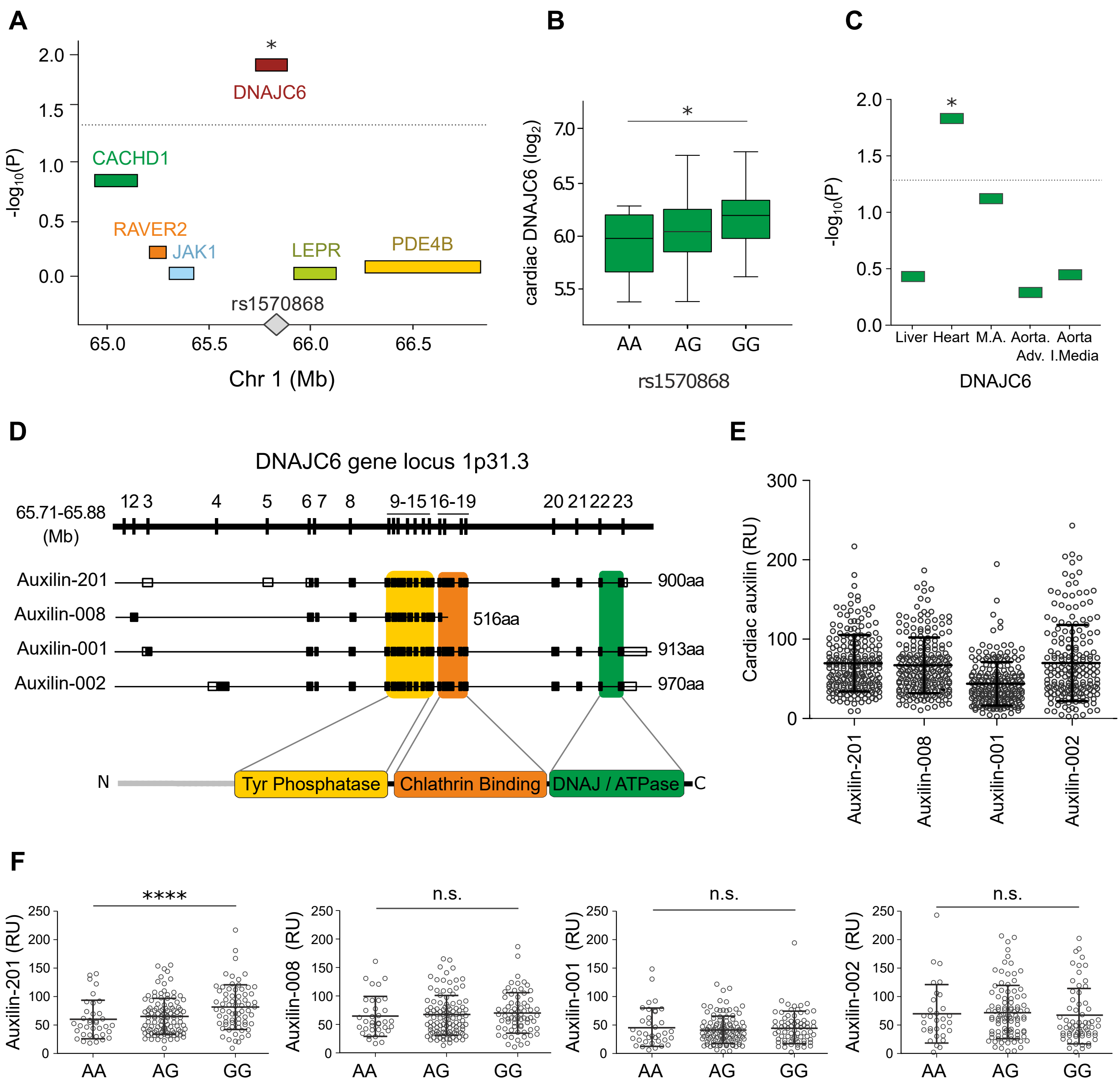

Figure 2 Identification of *DNAJC6* (*auxilin*) as a novel fetal genetic risk factor for CHB. (A) Effect of rs1570868 genotype on cardiac expression of genes located within a 1 Mb interval centred on rs1570868 (chromosomal position 1p31.3). (B) Cardiac *DNAJC6* expression stratified by rs1570868 genotypes. Allele frequency: 0.416 (A) and 0.584 (G) (n=101), β=0.066. (C) Effect of rs1570868 genotype on *DNAJC6* expression in different tissues. Liver (n=151), heart (n=101), m.a.; mammary artery (n=88), aorta AdV.; aorta adventia (n=90), aorta I. media; aorta intima media (n=104). An additive linear regression model was applied (A–C). Dashed line indicates p=0.05. (D) *DNAJC6* gene locus and predicted protein-coding auxilin transcript variants and functional domains. (E, F) Cardiac expression of auxilin transcript variants (E), stratified according to rs1570868 genotype (F), relative to cardiac β2-microglobulin expression (n=217). Results are shown as mean±SD. Linear regression analysis was applied. *P<0.05, ****p<0.0001. n.s, not significant.

Auxilin deficiency impairs cardiac cell connectivity and disturbs calcium homoeostasis

We next set out to investigate the role of auxilin in cardiac function using auxilin-deficient mice. We first confirmed that auxilin is indeed expressed in wild-type mouse neonatal heart (figure 4A), and also verified its described, high expression in mouse brain (figure 4B). In line with our findings of high fetal cardiac auxilin expression in human tissue, we observed that cardiac auxilin expression in the mouse also peaks in fetal heart tissue (figure 4C and online supplemental figure 3J,K), and verified that auxilin localises to vesicular structures partly colocalising with clathrin also in cultured neonatal mouse cardiomyocytes (figure 4D,E).

Ca^{2+} is one of the main regulators of cardiomyocyte function, and to evaluate the impact of auxilin deficiency on cardiomyocyte performance we analysed spontaneous $(Ca^{2+})_i$ oscillations in primary cultures of wild-type and auxilin knockout neonatal cardiomyocytes using the calcium sensitive fluorescent dye

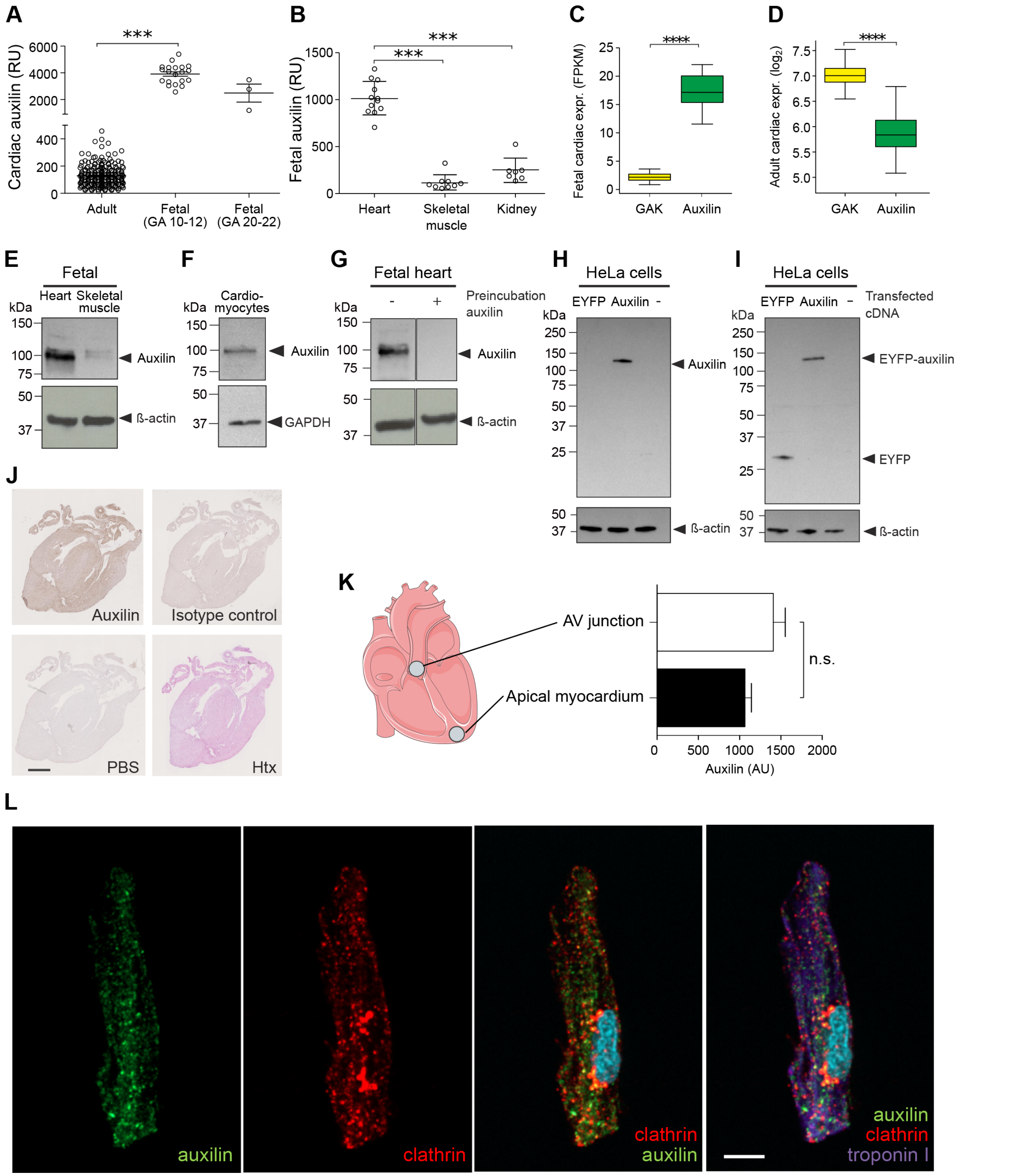

Figure 3 Auxilin is expressed in the human fetal heart and co-localises with clathrin in primary cardiomyocytes. (A) Auxilin cardiac expression in human adult (n=217) and fetal tissue, gestational age (GA) 10–12 weeks (n=20) and 20–22 weeks (n=3). (B) Auxilin expression in human fetal heart (n=12), skeletal muscle (n=9), and kidney (n=7), GA 10–12 weeks. auxilin expression relative to β2-microglobulin expression (A, B). (C) Human cardiac expression of GAK and auxilin in fetal tissue, GA 10–12 weeks (n=32). (D) Human cardiac expression of GAK and auxilin in adult tissue (n=127). (E) Auxilin protein expression in human fetal heart and skeletal muscle. (F) Auxilin protein expression in human cardiomyocytes differentiated from iPS cells. (G) Antibody specificity verified by preincubation with recombinant auxilin before Western blot of human fetal heart. (H, I) Immunoblotting with anti-auxilin (H) and anti-EYFP (I) of HeLa cell lysates transfected with recombinant EYFP (EYFP) or EYFP-auxilin (auxilin) or untransfected (-). (J) ubiquitous expression of auxilin detected by immunohistochemistry in sections of paraformaldehyde-fixed, paraffin-embedded human fetal cardiac tissue, GA 12 weeks. Scale bar represents 1 mm. (K) Auxilin mRNA expression within the apical myocardial and AV junctional tissue after microdissection of human fetal hearts (n=6; gestational age 20–22 weeks). (L) Subcellular localisation of auxilin and clathrin in cultured primary human fetal cardiomyocytes, GA 22 weeks. Counterstain by DAPI to visualise the nucleus (cyan). Scale bar represents 7.9 µm. Results are shown as mean±SE; Mann-Whitney U test. ***p<0.001, ****p<0.0001. AV, atrioventricular;

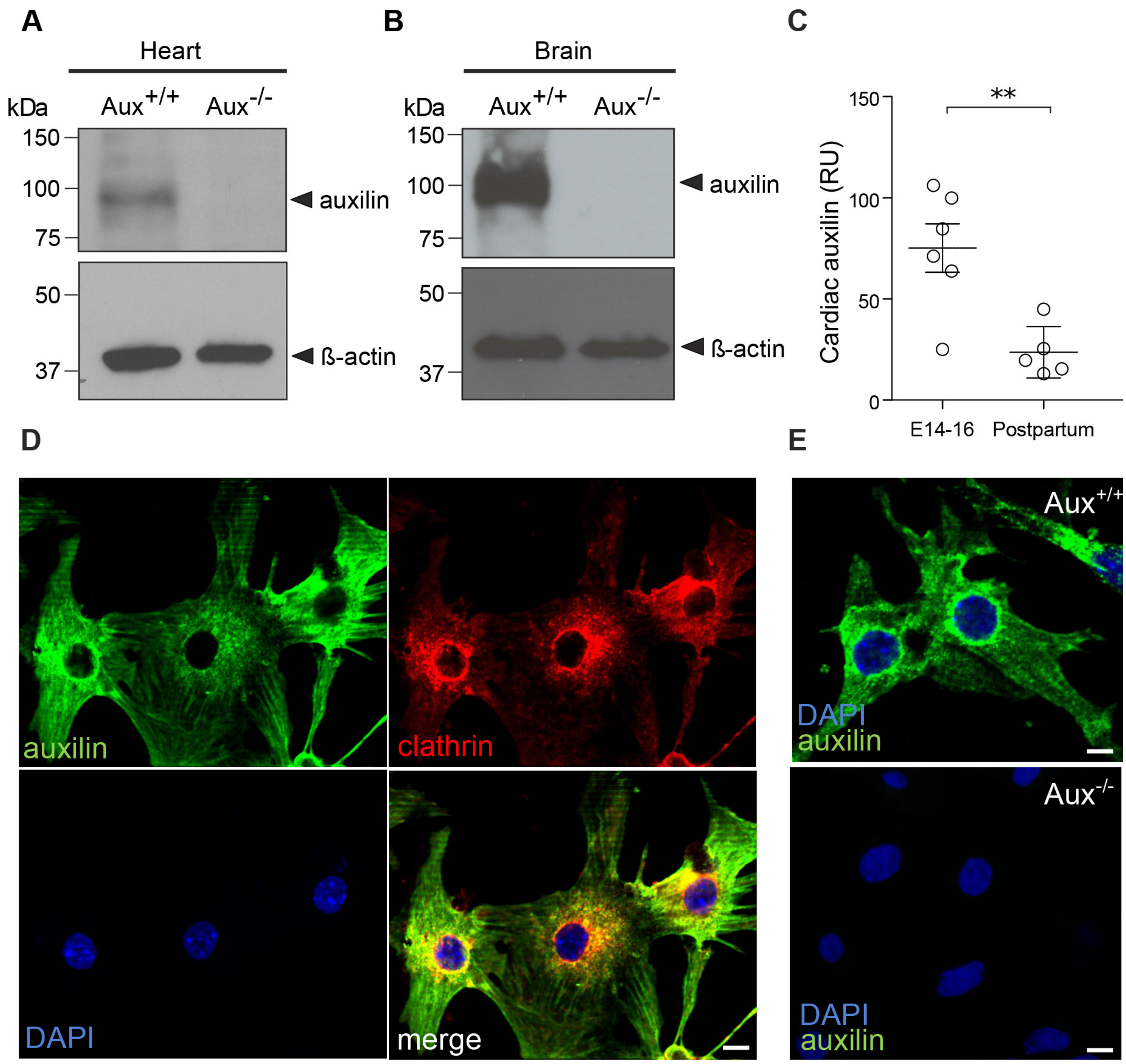

Figure 4 Auxilin is expressed in the mouse neonatal and fetal heart and colocalises with clathrin in primary cardiomyocytes. (A, B) Auxilin protein expression in the heart (A) and brain (B) of neonatal mice. Upper panel: auxilin; lower panel: β-actin. (C) Cardiac RNA expression of auxilin in mouse fetuses E14-E16 (n=6) and pups post partum (n=5). Expression levels are relative to TAF8 expression. (D) Subcellular localisation of auxilin and clathrin in cultured primary neonatal mouse cardiomyocytes. Scale bar represents 20 µm. (E) Immunofluorescence staining of cultured wild-type or auxilin knockout primary neonatal mouse cardiomyocytes using anti-auxilin antibody HPA031182, 1:200. Results are shown as mean±SE; two-tailed Student's t-test, **p<0.01.

(Fluo-4-AM) and time lapse imaging. Auxilin-deficient cardiomyocytes presented a pronounced irregular oscillation pattern (figure 5A,B and online supplemental movies 1 and 2), with reduced mean frequency and increased variability of $(Ca^{2+})_i$ oscillations compared with wild-type cells (figure 5C,D), though the total number or number of Ca-oscillating cells per area did not differ between wild-type and auxilin-deficient cultures (figure 5E). Strikingly, auxilin-deficient cells also appeared unable to organise into well-connected cellular networks in vitro, in contrast to wild-type cells (figure 5F). Cross-correlation analysis of cardiomyocyte $(Ca^{2+})_i$ activity demonstrated lower connectivity among auxilin-deficient cells (figure 5G), as well as a decreased mean path length reflecting an impaired capacity to communicate with cells at greater distances (figure 5H). Auxilin-deficient cells were, however, capable of interacting in so-called small-world networks (figure 5I).

Auxilin deficiency leads to decreased cell surface expression of the calcium channel $Ca_v1.3$ on cardiocytes

Given the described role of auxilin in the clathrin-mediated endocytic process and our finding that auxilin-deficient cardiomyocytes display a disturbed calcium homoeostasis, we hypothesised that absence of auxilin may impair the recycling of calcium channels to the plasma membrane of cardiomyocytes. Flow cytometry analysis of mouse neonatal Sirpa$^+$ cardiocytes revealed that the proportion of cells expressing the calcium channel $Ca_v1.3$ was comparable in auxilin-deficient and wild-type mice (figure 6A and B), but that $Ca_v1.3$ cell surface expression was significantly lower in Sirpa$^+$$Ca_v1.3^+$ auxilin-deficient cells compared with wild-type cells (p<0.01, figure 6C). Conversely, cardiac expression levels of $Ca_v1.3$ RNA transcripts were significantly higher in auxilin-deficient neonatal mice compared with wild-type mice (figure 6D), indicating that decreased $Ca_v1.3$ expression

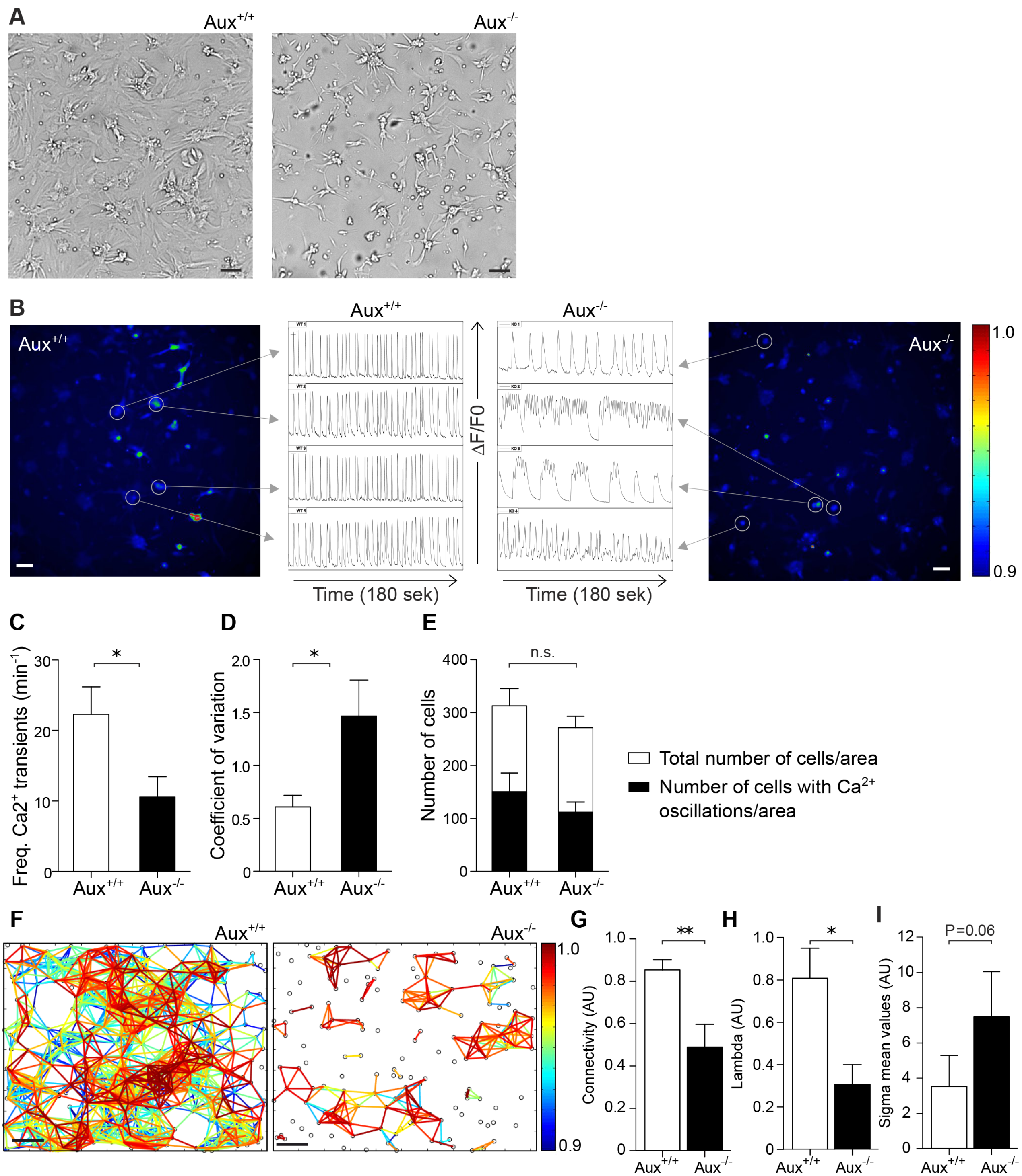

Figure 5 Auxilin deficiency causes impaired calcium homoeostasis and decreased intercellular connectivity in neonatal primary cardiomyocytes. (A) Phase-contrast images of primary neonatal cardiomyocytes of wild type and auxilin knockout mice in cultured monolayers. (B) Time lapse images of $(Ca^{2+})_i$ transients in spontaneously oscillating cardiomyocytes isolated from neonatal mice and loaded with Fluo4-AM. Examples of $(Ca^{2+})_i$ recordings from individual cardiomyocytes are shown. Videos of these cultures presented in online supplemental movie 2. (C, D) Frequency of $(Ca^{2+})_i$ oscillation transients and coefficient of variation in wild-type and knockout neonatal cardiomyocytes. Data are based on measurements from n=7 (wild-type) and n=6 (auxilin-knockout independent experiments with a mean of 165 cells analysed per experiment, each conducted with cells pooled from littermates (≥5 pups). (E) $(Ca^{2+})_i$ transients measurements in neonatal cardiomyocyte cultures showing the number of cells with $(Ca^{2+})_i$ transients per area and the total number of cells per area from wild-type vs auxilin knockout mouse pups. (F) Functional cell connection maps illustrating significantly correlated, thus connected, pairs of representative cultured cardiomyocytes. Multicoloured bar indicates correlation coefficient, with higher values representing a stronger correlation between the activities of the cells connected by the line. (G) Connectivity index in neonatal cardiomyocytes. (H) Lambda index representing the shortest mean path length in neonatal cardiomyocytes. (G–I) Representation of cardiomyocyte organisation into small-world networks in wild-type vs knockout cultures. Data are based on measurements from n=7 (wild-type) and n=6 (auxilin-knockout) independent experiments with a mean of 165 cell analysed per experiment, each conducted with cells pooled from littermates (≥5 pups). Au: arbitrary units. scale bars 100 µm. Results are shown as mean±SE; two-tailed Student's t-test, *p<0.05, **p<0.01.

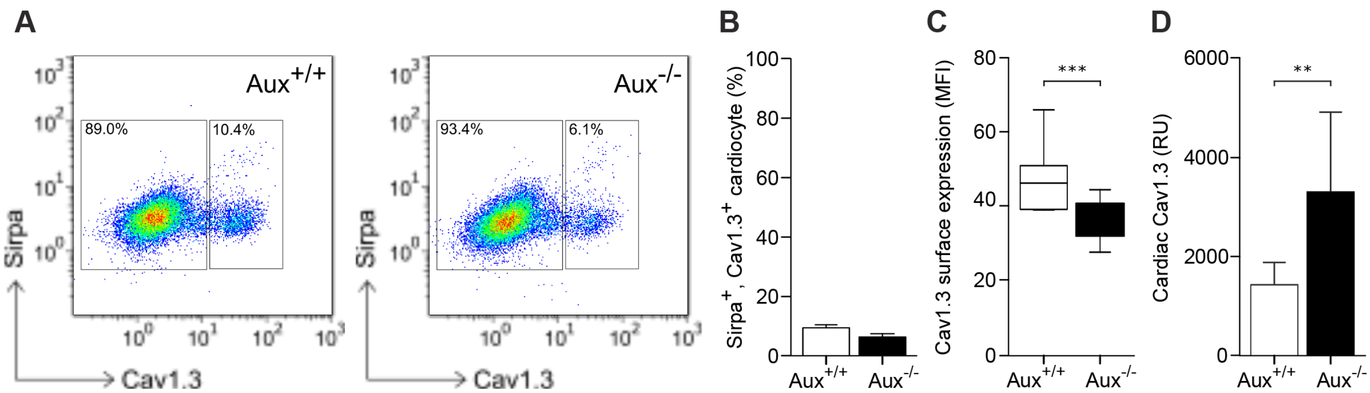

Figure 6 Auxilin deficiency leads to decreased cell surface expression of the $Ca_v1.3$ calcium channel in primary neonatal cardiomyocytes. (A, B) Flow cytometry analysis of wild-type and auxilin-deficient SIRPa and $Ca_v1.3$ double-stained primary mouse neonatal cardiomyocytes. (C) Mean fluorescence intensity (MFI) of $Ca_v1.3$ cell surface expression in $Sirpa^+Ca_v1.3^+$ primary neonatal cardiomyocytes from wild-type vs auxilin-deficient mice. Calculations are based on n=9 independent experiments per genotype with pooled cells from littermates (≥5 pups per experiment). (D) Cardiac RNA expression of $Ca_v1.3$ in primary neonatal cardiocytes from wild-type (n=5) and auxilin-deficient mice (n=5). Expression levels are relative to cardiac TAF8 expression. Results are shown as mean±SEM or minimal and maximal values; Mann-Whitney test, **p<0.01, ***p<0.001.

on the plasma membrane of auxilin-deficient cells was not due to a general decrease in expression, and further suggesting that auxilin-deficient cardiomyocytes upregulate the transcription of $Ca_v1.3$ to compensate for decreased protein levels on the cell surface.

Auxilin-deficient mice display Chb abnormalities during fetal development

To address whether the lack of auxilin affects fetal heart function in vivo, we monitored developing mice in utero by Doppler echocardiography. Notably, we observed several different CHB-related cardiac pathologies in auxilin-deficient mice at the fetal stage (figure 7A–F, online supplemental movies 3 and 4). Both the AV-time and isovolumetric contraction time were prolonged in auxilin knockout fetuses compared with wild-type fetuses (figure 7G,H). Furthermore, auxilin-deficient fetuses displayed abnormal heart rates and arrhythmias, including frequent ectopic beats generated in the atria and/or ventricles (figure 7I,J and online supplemental table 4). Interestingly, the effect was gene-dosage dependent as heterozygous animals showed an intermediate phenotype (figure 7G–J). Of note, the number of ectopic beat observations among auxilin knockout animals peaked at gestational day 13 (figure 7K), which corresponds to the window of disease onset for CHB in humans. Importantly, the cardiac abnormalities we observed in auxilin-deficient mice in utero are similar to those observed in human fetuses with CHB, as exemplified by one of our recorded human fetal case presenting with ectopic tachycardia at gestational age 21 weeks (figure 7L,M), and progressing to CHB at gestational age 24 weeks (figure 7N,O, online supplemental movies 5 and 6).

DISCUSSION

Given the low recurrence rate of CHB despite the persistence of autoantibodies in the mothers, fetal genetic factors have been suggested to contribute to disease development. Here, we identify auxilin/*DNAJC6* as a novel fetal susceptibility gene for CHB and report that decreased cardiac expression associates with the disease genotype. We further demonstrate that auxilin under normal circumstances is highly expressed in the fetal heart, and that auxilin deficiency impairs cardiomyocyte performance in vitro and leads to cardiac CHB abnormalities in vivo, thereby directly linking a novel susceptibility gene with disease mechanism and providing a functional basis for how decreased expression of auxilin may contribute to the development of CHB.

The majority of mothers of children with CHB carry autoantibodies to the Ro/SSA autoantigens and will thus have genetic traits reflecting their autoimmune status.[25 26] In order to segregate these potentially confounding maternal disease traits and identify genetic traits specific to CHB, we chose to perform a genome-wide association study using a family-based setup including individuals with CHB and their unaffected first-degree relatives. Interestingly, we found that the SNPs most significantly associated with CHB were located outside the human leucocyte antigen (HLA) region, in contrast to a previously published genome-wide association study in which the SNPs most significantly associated with CHB were found in the HLA region.[27] This discrepancy may be explained by the fact that the latter study[27] was based on a C-C set-up, and that its findings may therefore reflect inherited maternal traits linked to the autoimmune status of the mothers rather than CHB-specific disease traits.

Our family-based analysis strategy uncovered several CHB-specific polymorphisms across the whole genome, and additional validation of association combined with cardiac eQTL analysis identified auxilin/*DNAJC6* as the primary candidate for a susceptibility gene for CHB. This prompted us to further investigate the auxilin expression pattern. Indeed, auxilin expression and function had mainly been described in neuronal tissue,[28 29] and its potential involvement in heart function was unknown. Surprisingly, we found that auxilin was not only expressed in the heart, but that its levels were also markedly higher in fetal compared with adult cardiac tissue. In addition, we observed that the homologous protein GAK, which has been suggested to act as a functional substitute for auxilin,[30] was expressed only at low levels in the fetal heart, but at higher levels than auxilin in the adult heart. These findings, therefore, provide a rationale as to why a decreased expression of auxilin would be associated with a fetal cardiac phenotype.

Auxilin operates in the clathrin-mediated endocytic process,[31] and absence of auxilin may therefore impair the recycling of ion channels or other molecules important for cardiac function to the plasma membrane of cardiomyocytes. This in turn could explain the lower cellular connectivity and communication as well as the decreased and less well-coordinated Ca^{2+} oscillations we observed in auxilin-deficient cardiomyocytes.

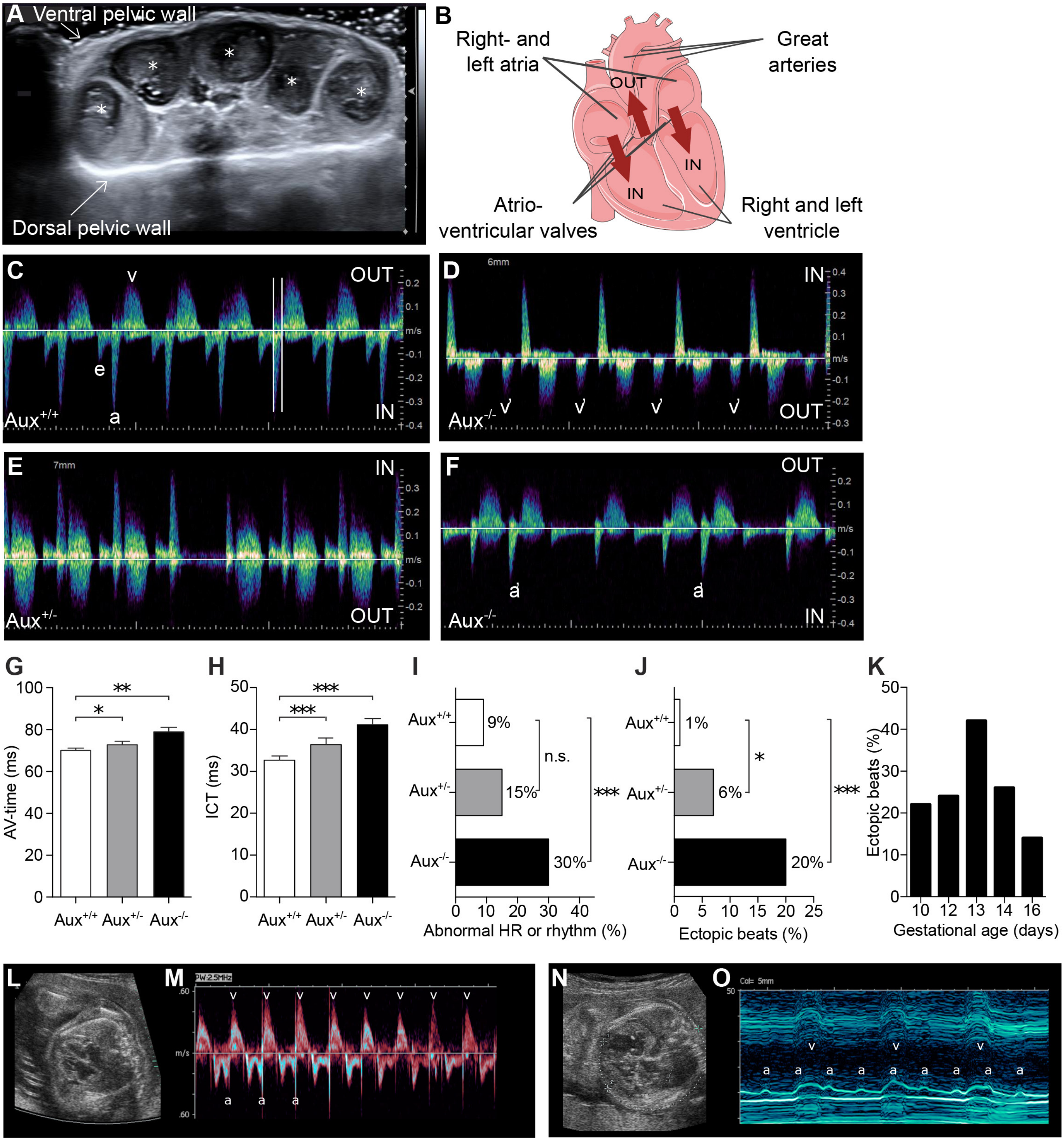

Figure 7 Auxilin deficiency causes cardiac abnormalities in vivo during fetal development. (A) Transsectional abdominal ultrasound view showing individual mouse fetuses (*) in utero. (B) Illustration of spatial and directional relationships between ventricular inflows and outflows registered in (C–F). (C–F) Echocardiographic Doppler flow velocity recordings from wild-type and auxilin-deficient fetuses, with cardiac inflow (IN) through atrioventricular valves and outflow (OUT) in the great arteries. (C) Normal recording showing two-peaked inflow with early passive e-wave (e), higher a-wave (a), and ventricular outflow (v). Vertical lines denote one AV-time interval. (D) Ventricular ectopic beats (VES) (v′) in bigeminy. (E) Mobitz type II, second-degree AV-block. (F) Conducted premature ectopic supraventricular beats (SVES) (a′). (G, H) mechanical AV-time interval and isovolumetric contraction time (ICT), Kruskal-Wallis and Dunn's post hoc tests. Results are shown as mean±SE. (I, J) Proportion of fetuses with abnormal heart rate (HR) or rhythm (I), or with ectopic beats (SVES, VES) (J), χ^2 test. Auxilin$^{+/+}$ (n=147), auxilin$^{+/-}$ (n=89), and auxilin$^{-/-}$ (n=131) fetuses (G–J). (K) percentages of auxilin$^{-/-}$ fetuses with ectopic beats according to gestational age. Percentages are calculated based on the total number of auxilin$^{-/-}$ fetuses at each gestational age. l-o a human fetal case of junctional ectopic tachycardia progressing to CHB. (L, M) normal appearing heart with ectopic tachycardia at gestational age (GA) 21 weeks. (N, O) Complete CHB at GA 24 weeks with bradycardia and dilated echogenic heart. *P<0.05, **p<0.01, ***p<0.001.

In support of this hypothesis, we found that auxilin-deficient cardiac cells displayed lower levels of the calcium channel $Ca_v1.3$ on their plasma membrane compared with wild-type cells. Interestingly, $Ca_v1.3$-deficient mice have been reported to exhibit cardiac abnormalities such as sinus bradycardia and AV block at birth,[32 33] suggesting that decreased expression of $Ca_v1.3$ on the surface of auxilin-deficient cells may contribute in part to the cardiac abnormalities we observed in auxilin-deficient mice in utero. Indeed, we show here that auxilin-deficient mice develop cardiac abnormalities in utero similar to early CHB manifestations, such as ectopic beats, arrhythmias and prolongation of the AV time. AVBII/III was observed, but the occurrence did not reach statistical significance.

Calcium channels, including $Ca_v1.3$, have been described as potential targets of autoantibodies from mothers of children with CHB,[34–36] and maternal antibodies were reported to inhibit $Ca_v1.3$ calcium currents in exogenous expression systems.[34] A genetically determined lower cardiac auxilin expression, resulting in decreased calcium channel presence on the cell surface, may thus synergize with the inhibitory effect of maternal autoantibodies to further diminish $I_{Ca,L}$ current density and overall cardiomyocyte performance. Interestingly, fetal cardiomyocytes do not yet possess a fully developed sarcoplasmic reticulum, and the excitation-contraction coupling is thus largely dependent on cell surface calcium channels.[37 38] By contrast, adult cardiac cells rely mainly on sarcoplasmic calcium stores. Decreased expression of auxilin resulting in lower surface expression of calcium channels would therefore have a larger impact on cardiomyocyte function in the fetal heart than in the adult heart, rendering fetal cardiac cells particularly susceptible to the pathogenic effects of maternal antibodies while maternal cardiac cells are left relatively unaffected. This in turn might begin to explain why, despite the presence of circulating autoantibodies, cardiac manifestations similar to CHB are not detected in mothers of children with CHB.

Considering the role of auxilin in the clathrin-mediated endocytosis process, it is probable that auxilin deficiency may affect the presence of many different molecules to the plasma membrane of cardiac cells. Here, we limited our investigation to the $Ca_v1.3$ calcium channel as a proof of concept; however, it is likely that auxilin deficiency alters the surface expression also of other molecules, such as other ion channels or connexins involved in cardiac function, which in turn may contribute to CHB development. In addition, although we here focus on auxilin/*DNAJC6* as a susceptibility gene for CHB, it is likely that other genetic variants may contribute directly or indirectly to cardiomyocyte performance and hence also affect susceptibility to CHB. However, CHB is a rare disease in the general population, occurring in about 1 in 20 000 births,[21] and establishing large cohorts of patients that would enable the detection of many different risk variant combinations remains a challenge. The main limitations of this study are linked to this rarity of the studied condition, and includes the employed threshold at $p \leq 1 \times 10^{-4}$ for the family-based association for disease traits and the lack of a replication cohort of patients with CHB.

In all, we identify auxilin/DNAJC6 as a novel susceptibility gene for CHB and demonstrate a previously unreported role for auxilin in fetal cardiac function, revealing in particular that auxilin is necessary for cardiac cells to maintain normal calcium homoeostasis and establish functional networks. The disease-associated genetic variant, leading to decreased auxilin expression, may thus affect fetal myocardial function, both mechanically and electrically, as part of CHB. The involvement of maternal autoantibodies in CHB has long been recognised, especially regarding the establishment of inflammation and subsequent scaring of the AV node.[39 40] However, the mechanisms underlying the early phases and cardiac manifestations of NLE other than complete AV block remain unclear.[41] Importantly, we show here that auxilin-deficient mice develop cardiac abnormalities in utero similar to CHB manifestations such as prolonged AV time interval and isovolumetric contraction time, ectopic beats and arrhythmias, and provide a mechanistic basis as to how lack of auxilin may underlie such features at the molecular and cellular level. Identification of auxilin/DNAJC6 as a susceptibility gene for CHB that directly impacts cardiac function therefore begins to elucidate the tissue-dependent pathogenic mechanisms involved in CHB. This, in turn, shifts the focus from solely trying to prevent the pathogenic effects of maternal antibodies and instead taking into account intrinsic cardiac defects affecting fetal heart function, thus opening the road to conceiving new screening and therapeutic strategies for this often lethal condition.

Author affiliations
[1]Department of Medicine, Karolinska Institutet, Karolinska University Hospital, Stockholm, Sweden
[2]Technical University of Denmark, Lyngby, Denmark
[3]Department of Women's and Children's Health, Karolinska Institutet, Stockholm, Sweden
[4]Department of Physiology and Experimental Medicine, Hospital for Sick Children, Washington, DC, USA
[5]Department of Clinical Neuroscience, Karolinska Institutet, Stockholm, Sweden
[6]Pediatric Cardiology, Hospital for Sick Children, Toronto, Ontario, Canada
[7]Department of Molecular Medicine and Surgery, Karolinska Institutet, Stockholm, Sweden
[8]National Institutes of Health, Bethesda, Maryland, USA
[9]Evergrande Center for Immunologic Diseases, Harvard Medical School, Boston, Massachusetts, USA
[10]Broegelmann Research Laboratory, Department of Clinical Science, University of Bergen, Bergen, Norway

Correction notice This article has been corrected since it was first published. The open access licence has been updated to CC BY.

Acknowledgements We thank Amina Ossoinak for excellent technical support.

Collaborators The Swedish congenital heart block study group: Aurelie Ambrosi, Amanda Skog Andreasson, Gunnar Bergman, Håkan Eliasson, Eva Fernlund, Fredrik Gadler, Anders Jonzon, Ingrid Kockum, Linda Lagnefeldt, Malin Hedlund, Mats Mellander, Sabrina Meisgen, Johannes Mofors, Vijole Ottosson, Annika Rydberg, Stina Salomonsson, Thomas Skogh, Sven-Erik Sonesson, Elke Theander, Joanna Tingström, Guðný Ella Thorlacius, Marie Wahren-Herlenius, Annika Öhman.

Contributors SM and MW-H designed the study with input from MH, AA, VKK, EH, AE, IK and S-ES. Members of TSCHBSG, AF-C, AH, TO, PE, JM and KG-D assisted in identification and characterisation of patients and controls. LG and RMH provided study material. SM, MH, VO, LB, LS, SR, LM, WN and S-ES performed the experiments. SM, MH, LF, GET, VO, DR, DF, LB, JM, EH, IK and S-ES analysed the data. SM, AA, GET and MW-H wrote the manuscript, and all authors participated in manuscript preparation until its final form. MW-H is the study guarantor.

Funding The study was supported by grants from the Swedish Research Council, the Heart-Lung Foundation, the Stockholm County Council, Karolinska Institutet, the Swedish Rheumatism Association, King Gustaf the V:th 80-year Foundation, the Freemason Children Foundation Stockholm and the Torsten and Ragnar Söderberg Foundation.

Competing interests TO has received unrestricted multiple sclerosis research grants, honoraria for advisory boards/lectures from Biogen, Novartis, Merck, Sanofi and Roche. Other authors declare no competing interests.

Patient and public involvement Patients and/or the public were not involved in the design, or conduct, or reporting, or dissemination plans of this research.

Patient consent for publication Not applicable.

Ethics approval The studies were approved by the Regional Ethical Committee, Karolinska Institutet, Stockholm, Sweden.

Provenance and peer review Not commissioned; externally peer reviewed.

Data availability statement Data are available on reasonable request. There are online supplemental files containing data.

ORCID iD
Marie Wahren-Herlenius http://orcid.org/0000-0002-0915-7245

REFERENCES

1 Buyon JP, Ben-Chetrit E, Karp S, *et al*. Acquired congenital heart block. Pattern of maternal antibody response to biochemically defined antigens of the SSA/Ro-SSB/La system in neonatal lupus. *J Clin Invest* 1989;84:627–34.
2 McCauliffe DP. Neonatal lupus erythematosus: a transplacentally acquired autoimmune disorder. *Semin Dermatol* 1995;14:47–53.
3 Salomonsson S, Strandberg L. Autoantibodies associated with congenital heart block. *Scand J Immunol* 2010;72:185–8.
4 Hutter D, Silverman ED, Jaeggi ET. The benefits of transplacental treatment of isolated congenital complete heart block associated with maternal anti-Ro/SSA antibodies: a review. *Scand J Immunol* 2010;72:235–41.
5 Sonesson S-E, Wahren-Herlenius M. Mortality in congenital heart block. *Lancet Rheumatol* 2020;2:e588–9.
6 Levesque K, Morel N, Maltret A, *et al*. Description of 214 cases of autoimmune congenital heart block: results of the French neonatal lupus syndrome. *Autoimmun Rev* 2015;14:1154–60.
7 Eronen M, Sirèn MK, Ekblad H, *et al*. Short- and long-term outcome of children with congenital complete heart block diagnosed in utero or as a newborn. *Pediatrics* 2000;106:86–91.
8 Brucato A, Previtali E, Ramoni V, *et al*. Arrhythmias presenting in neonatal lupus. *Scand J Immunol* 2010;72:198–204.
9 Hornberger LK, Al Rajaa N. Spectrum of cardiac involvement in neonatal lupus. *Scand J Immunol* 2010;72:189–97.
10 Bergman G, Eliasson H, Bremme K, *et al*. Anti-Ro52/SSA antibody-exposed fetuses with prolonged atrioventricular time intervals show signs of decreased cardiac performance. *Ultrasound Obstet Gynecol* 2009;34:543–9.
11 Sonesson S-E, Salomonsson S, Jacobsson L-A, *et al*. Signs of first-degree heart block occur in one-third of fetuses of pregnant women with anti-SSA/Ro 52-kd antibodies. *Arthritis Rheum* 2004;50:1253–61.
12 Kurita T, Ohe T, Marui N, *et al*. Bradycardia-induced abnormal QT prolongation in patients with complete atrioventricular block with torsades de pointes. *Am J Cardiol* 1992;69:628–33.
13 Jaeggi ET, Hamilton RM, Silverman ED, *et al*. Outcome of children with fetal, neonatal or childhood diagnosis of isolated congenital atrioventricular block. A single institution's experience of 30 years. *J Am Coll Cardiol* 2002;39:130–7.
14 Moak JP, Barron KS, Hougen TJ, *et al*. Congenital heart block: development of late-onset cardiomyopathy, a previously underappreciated sequela. *J Am Coll Cardiol* 2001;37:238–42.
15 Villain E, Coastedoat-Chalumeau N, Marijon E, *et al*. Presentation and prognosis of complete atrioventricular block in childhood, according to maternal antibody status. *J Am Coll Cardiol* 2006;48:1682–7.
16 Zhao H, Cuneo BF, Strasburger JF, *et al*. Electrophysiological characteristics of fetal atrioventricular block. *J Am Coll Cardiol* 2008;51:77–84.
17 Salomonsson S, Dzikaite V, Zeffer E, *et al*. A population-based investigation of the autoantibody profile in mothers of children with atrioventricular block. *Scand J Immunol* 2011;74:511–7.
18 Ambrosi A, Salomonsson S, Eliasson H, *et al*. Development of heart block in children of SSA/SSB-autoantibody-positive women is associated with maternal age and displays a season-of-birth pattern. *Ann Rheum Dis* 2012;71:334–40.
19 Brito-Zerón P, Izmirly PM, Ramos-Casals M, *et al*. The clinical spectrum of autoimmune congenital heart block. *Nat Rev Rheumatol* 2015;11:301–12.
20 Kan N, Silverman ED, Kingdom J, *et al*. Serial echocardiography for immune-mediated heart disease in the fetus: results of a risk-based prospective surveillance strategy. *Prenat Diagn* 2017;37:375–82.
21 Sonesson S-E, Ambrosi A, Wahren-Herlenius M. Benefits of fetal echocardiographic surveillance in pregnancies at risk of congenital heart block: single-center study of 212 anti-Ro52-positive pregnancies. *Ultrasound Obstet Gynecol* 2019;54:87–95.
22 Meisgen S, Östberg T, Salomonsson S, *et al*. The HLA locus contains novel foetal susceptibility alleles for congenital heart block with significant paternal influence. *J Intern Med* 2014;275:640–51.
23 Ainsworth HC, Marion MC, Bertero T, *et al*. Association of natural killer cell ligand polymorphism HLA-C Asn80Lys with the development of Anti-SSA/Ro-Associated congenital heart block. *Arthritis Rheumatol* 2017;69:2170–4.
24 Kyriakidis NC, Kockum I, Julkunen H, *et al*. European families reveal MHC class I and II associations with autoimmune-mediated congenital heart block. *Ann Rheum Dis* 2018;77:1381–2.
25 Lessard CJ, Li H, Adrianto I, *et al*. Variants at multiple loci implicated in both innate and adaptive immune responses are associated with Sjögren's syndrome. *Nat Genet* 2013;45:1284–92.
26 International Consortium for Systemic Lupus Erythematosus Genetics (SLEGEN), Harley JB, Alarcón-Riquelme ME, *et al*. Genome-wide association scan in women with systemic lupus erythematosus identifies susceptibility variants in ITGAM, PXK, KIAA1542 and other loci. *Nat Genet* 2008;40:204–10.
27 Clancy RM, Marion MC, Kaufman KM, *et al*. Identification of candidate loci at 6p21 and 21q22 in a genome-wide association study of cardiac manifestations of neonatal lupus. *Arthritis Rheum* 2010;62:3415–24.
28 Ahle S, Ungewickell E. Auxilin, a newly identified clathrin-associated protein in coated vesicles from bovine brain. *J Cell Biol* 1990;111:19–29.
29 Yim Y-I, Sun T, Wu L-G, *et al*. Endocytosis and clathrin-uncoating defects at synapses of auxilin knockout mice. *Proc Natl Acad Sci U S A* 2010;107:4412–7.
30 Greener T, Zhao X, Nojima H, *et al*. Role of cyclin G-associated kinase in uncoating clathrin-coated vesicles from non-neuronal cells. *J Biol Chem* 2000;275:1365–70.
31 Ungewickell E, Ungewickell H, Holstein SE, *et al*. Role of auxilin in uncoating clathrin-coated vesicles. *Nature* 1995;378:632–5.
32 Karnabi E, Qu Y, Mancarella S, *et al*. Rescue and worsening of congenital heart block-associated electrocardiographic abnormalities in two transgenic mice. *J Cardiovasc Electrophysiol* 2011;22:922–30.
33 Platzer J, Engel J, Schrott-Fischer A, *et al*. Congenital deafness and sinoatrial node dysfunction in mice lacking class D L-type Ca2+ channels. *Cell* 2000;102:89–97.
34 Qu Y, Baroudi G, Yue Y, *et al*. Novel molecular mechanism involving alpha1D (Cav1.3) L-type calcium channel in autoimmune-associated sinus bradycardia. *Circulation* 2005;111:3034–41.
35 Qu Y, Xiao GQ, Chen L, *et al*. Autoantibodies from mothers of children with congenital heart block downregulate cardiac L-type Ca channels. *J Mol Cell Cardiol* 2001;33:1153–63.
36 Strandberg LS, Cui X, Rath A, *et al*. Congenital heart block maternal sera autoantibodies target an extracellular epitope on the α1G T-type calcium channel in human fetal hearts. *PLoS One* 2013;8:e72668.
37 Brillantes AM, Bezprozvannaya S, Marks AR. Developmental and tissue-specific regulation of rabbit skeletal and cardiac muscle calcium channels involved in excitation-contraction coupling. *Circ Res* 1994;75:503–10.
38 Fisher DJ. Recent insights into the regulation of cardiac Ca2+ flux during perinatal development and in cardiac failure. *Curr Opin Cardiol* 1995;10:44–51.
39 Clancy RM, Kapur RP, Molad Y, *et al*. Immunohistologic evidence supports apoptosis, IgG deposition, and novel macrophage/fibroblast crosstalk in the pathologic cascade leading to congenital heart block. *Arthritis Rheum* 2004;50:173–82.
40 Litsey SE, Noonan JA, O'Connor WN, *et al*. Maternal connective tissue disease and congenital heart block. Demonstration of immunoglobulin in cardiac tissue. *N Engl J Med* 1985;312:98–100.
41 Ambrosi A, Sonesson S-E, Wahren-Herlenius M. Molecular mechanisms of congenital heart block. *Exp Cell Res* 2014;325:2–9.

SUPPLEMENTAL MATERIAL

Auxilin is a novel susceptibility gene for congenital heart block which directly impacts fetal heart function

Meisgen S et al.

CONTENTS

SUPPLEMENTAL PATIENTS AND METHODS

Study populations, genotyping, and analysis

The cohort of patients diagnosed with congenital heart block and their families has been previously described,[1, 2] and clinical information is summarised in supplemental table 1. Confirmed maternal Ro/SSA autoantibodies were a prerequisite for inclusion and patients with major cardiac structural abnormalities, or postoperative or infection-induced block were excluded. DNA preparation and genotyping were performed on the Illumina 660W-Quad Beadchip. For family-based analysis, samples with an individual genotype call rate >95%, Mendelian errors per family <2%, SNP genotype call rate >95%, SNP Mendelian error <4%, minor allele frequency (MAF) >0.01 and Hardy-Weinberg equilibrium (HWE) $p>1x10^{-8}$ were included. The genomic inflation factor was $\lambda=1.01$ (supplemental figure 1). Association was calculated using the family-based association for disease trait (DFAM) analysis on the 534,192 SNPs included after quality control (QC) (NCBI build 36.3) in the 92 CHB cases and 256 non-affected family members using PLINK. P_{DFAM} values $\leq 1x10^{-4}$ were considered for further analysis. Risk allele and transmission frequencies, odds ratios, and confidence interval calculations were performed using PLINK. Genotyping data from population-based controls for the case-control analysis were obtained from the Swedish Multiple Sclerosis cohort,[3] n=527, and the Swedish section of the PROCARDIS study,[4] n=678. After QC with individual call rate >98%, SNP call rate >98%, MAF >0.05, HWE p>0.001, average Mendelian error rate 0.06% (CHB cohort) and IBD removal of out-of study controls with pHAT >0.12, 465,202 overlapping markers were included for further analysis. The genomic inflation factor was $\lambda=1.006$ (supplemental figure 1). After principal component analysis (PCA, EIGENSTRAT smartPCA[5]) we removed 13 population outliers (10 controls, 3 cases). In total, 1195 out-of-study controls and 89 cases were left for logistic regression analysis to confirm family-based SNP associations with CHB using the additive model and correcting for the only significant PC.

The studies were approved by the Regional Ethical Committee, Stockholm, Sweden. Participants or guardians gave informed written consent.

Study material

Samples for genotyping were collected as described above. Cardiac, mammary artery and aortic biopsy specimens were obtained from patients enrolled in the Advanced Study of Aortic Pathology (ASAP), described in,[6] and undergoing aortic valve surgery at the Karolinska University Hospital, Stockholm, Sweden. Fetal tissues from electively terminated normal pregnancies were collected at the Women´s and Children's Health Department, Karolinska University Hospital, Stockholm, Sweden and the Hospital for Sick Children, Toronto, Canada. The studies were approved by the Regional Ethical Committee, Karolinska Institutet, Stockholm, Sweden, and The Hospital for Sick Children, Toronto, Canada respectively. Participants gave informed written consent.

Expression quantitative trait loci analysis

Expression quantitative trait loci (eQTL) analysis was performed for disease-associated SNPs (dbSNP 130) and RNA expression data from the ASAP study population.[6] Microarray (Affymetrix GeneChip Human Exon Array 1.0) data were analyzed by R (version 2.14.2) using the RMA algorithm[7] in the Affymetrix Power Tools-1.12.0 package. Tests for association between genotype and log-transformed gene expression were performed using the additive model in R. Information on genes within the 1 Mb interval was retrieved from ENSEMBL release 58 (GRCh37).

Cardiac gene expression profiling

RNA sequencing was performed on an Illumina HiSeq 2500 System at 2x101 bp length and a depth of 64 to 115 million read pairs. The reads were aligned using STAR[8] to the hg38 assembly and gencode v21 exon-exon junctions, and FPKM (fragments per kilo base and million mapped reads) expression values were calculated using rpkmforgenes.py (http://sandberg.cmb.ki.se/rnaseq)[9] version 13, with settings -minqual 255 -rmnameoverlap -midread -fulltranscript and with RefSeq annotation. After QC and testing of cardiac-tissue specificity (FPKM *TNNT2*> 0), 32 samples remained.

Fetal cardiac microdissection and expression analysis

Total RNA of dissected human fetal heart AV junctional and apical myocardium tissue was extracted using the Qiagen RNeasy kit, quantified by Nanodrop and Bioanalyzer, labeled and applied onto the Affymetrix Human U133 plus 2 array. The results were normalized and analyzed by Partek® Genomics SuiteTM.

Experimental animals

Animals (auxilin$^{-/-}$ mice[10] and C57/BL6 (Jackson Laboratory, USA)) were kept and bred at the AKM animal facility at the Center for Molecular Medicine, Karolinska Institutet, Stockholm, Sweden. All experimental protocols were approved by the Ethics Committee Stockholm North.

Quantitative PCR and transcript alignment

Auxilin transcript-specific quantitative PCR analysis was performed using cDNA generated from total mRNA prepared from cardiac tissue biopsies of individuals enrolled in the ASAP study (n=224), from human fetal tissue and cultured iCell cardiomyocytes[2] (Cellular Dynamics International, Madison, WI, US) using the RNAeasy kit (Quiagen) and the SuperScript® III First-Strand Synthesis SuperMix (LifeTechnologies). For auxilin protein transcript alignment and the design of specific exon-exon spanning primers for the protein coding transcript variants auxilin-001, 002, 201, and 008, and for overall auxilin expression the ENSEMBL release 75 (GRCh37 assembly) was used. Primers used are listed in supplemental figure S2. For fetal tissue and iPS induced cardiomyocyte expression analysis, ABI gene expression assays were used. Quantitative PCR with 5ng template cDNA was performed using the iQ SYBR Green Supermix (Biorad, Sweden) or Taqman Universal Mastermix II NO UNG and the CFX384 Touch™ Real-Time PCR Detection System (Biorad, Sweden) using a two-step protocol (95°C for 10 minutes, followed by 95°C for 15 seconds and 60°C for 1 minute for 40 cycles). The amplification was performed in 384-well plates in duplicates and for SYBR PCR a standard curve was constructed using two-fold dilutions of pooled cDNA from five samples. Expression of genes of interest was normalized to β2-microglobulin or Taf8 using the delta Ct method.

Cloning of recombinant EYFP-auxilin

The auxilin-201 transcript was pcr amplified using a cdna library generated from human fetal heart (gestational week 12) and cloned into the peyfp-c1 vector (clontech). The construct was verified by sequencing. Primer sequences available upon request.

HeLa cell culturing and transfection

HeLa cells were plated in culture medium (DMEM supplemented with 10% FBS, 2 mM L-glutamine and 100 µg/mL Penicillin/Streptomycin) at a density of 250,000 cells/ml. Two hours after plating, transfection was performed by adding 100 µl DMEM, supplemented with 3µl X-tremeGene 9 DNA transfection agent (Roche) and 1 µg plasmid DNA (pEYFP-C1, pEYFP-auxilin) to each well. Cells were harvested 22 hours after transfection.

Western blot

Total cellular protein extracts were prepared by lyzing human fetal and neonatal mouse organs, cultured differentiated human cardiomyocytes (iCell Cardiomyocytes[2], Cellular Dynamics International, Madison, WI, US), Hela or Daudi cells in T-PER Tissue Protein Lysis buffer Reagent (Thermo Scientific) or CelLytic M Reagent (Sigma) supplemented with proteinase inhibitor cocktail (Thermo Scientific) using the Qiagen TissueRuptor for 2 minutes at 40 Hz. Total protein extracts were denatured by boiling for 5 minutes in 5% SDS sample buffer and loaded on a Mini-PROTEAN® TGX™ 4–15% precast linear gradient polyacrylamide gel (BioRad, Sweden). Size-separated proteins were blotted onto a nitrocellulose membrane. The membrane was blocked with 5% (w/v) fat-free milk 0.1% Tween 20-phosphate-buffered saline (TPBS) over night at 4°C. Membranes were washed with TPBS and incubated with a polyclonal anti-auxilin antibody (HPA031182 (Sigma) 1:250 for 1 hour at room temperature (RT), followed by incubation with horseradish peroxidase-conjugated anti-rabbit IgG (1:2000, DakoCytomation, Glostrup, Denmark) for 30 minutes at RT. Pre-incubation of the anti-auxilin antibody with 10 µg of the HPRR2550352 peptide (HPA project, Sweden) was performed for 1 hour at RT. Membranes were stripped by incubating in a 0.1 M NaOH solution for 15 minutes at RT to remove bound antibodies, subsequently washed with di-ionized water, and further incubated with anti-β-actin-HRP (1:50,000, Sigma) or anti-GAPDH-HRP (1:1000, Cell Signaling) for 1 hour at RT. All antibodies were diluted in 1% (w/v) fat-free milk in TPBS, and the membranes were washed in TPBS between incubations. Blots were developed with the ECL system (Amersham Biosciences, Little Chalfont, UK). Protein size was determined using the Precision Plus Protein™ Kaleidoscope Standards (BioRad, Sweden).

Meisgen S, *et al. Ann Rheum Dis* 2022;0:1–11. doi: 10.1136/annrheumdis-2021-221714

Immunohistochemistry staining

Tissue was fixed in 4% paraformaldehyde, paraffin-embedded, and sectioned with a microtome and placed on positively charged glass slides. The 8 µm sections were de-paraffinized by heating at 60°C for 18 hours, incubated in xylene twice for 5 minutes and rehydrated by immersing for 5 minutes into gradually diluted ethanol solutions (99, 95, and 70%), and thereafter washed in PBS. Antigen retrieval was performed by heating the slides in citrate solution (pH 6) at 98°C for 40 minutes, thereafter allowing slides to cool, and washing in water for 10 minutes. Slides were then consecutively treated at room temperature with 1% hydrogen peroxide for 30 minutes in the dark, avidin and biotin blocking solutions (VECTASTAIN) and 2% normal horse or goat serum for 20 minutes. Washing in PBS was performed between each step. Primary antibodies (2 µg/ml anti-auxilin (HPA031182, Sigma) or corresponding amount of isotype control (Negative control Rabbit Ig Fraction Ab, DakoCytomation) were added to the sections and incubated at RT for 60 minutes in a humidified chamber. After rinsing and washing in PBS, biotinylated goat-anti-rabbit or horse-anti-mouse IgG (1:750, DakoCytomation) diluted in PBS with 2% normal horse or goat serum was added to the sections and incubated for 60 minutes. The slides were then washed and treated with a pre-formed complex of biotin and peroxidase-labeled avidin (VECTASTAIN) for 45 minutes and then developed with the diaminobenzidine (DAB) kit (Vector) shielded from light for 10 minutes. Slides were counterstained with Mayer's hematoxylin and mounted with coverslips using Mountex (HistoLab, Gothenburg, Sweden). Sections were scanned with the Hamamatsu Nano Zoomer Slide Scanner and analyzed in the NPD View software.

Immunofluorescence staining of human fetal cardiac cells

After preparation, cells were fixed in 4% paraformaldehyde (PFA) for 10 minutes at 4°C and permeabilized in 0.1% (v/v) Triton-PBS buffer for 10 minutes at 4°C. Blocking was carried out using the permeabilization buffer supplemented with 2% (w/v) DSA and 1% (w/v) BSA for 1 hour at RT. Primary antibodies (goat anti-troponin I (Pierce), dilution 1:200; rabbit anti-auxilin (Labome), dilution 1:300; mouse anti-clathrin (Thermo Scientific), dilution 1:1,200) were diluted in blocking buffer and incubated for 2 hours at RT and shaking at 150 rpm. Cells were washed twice for 15 minutes with permeabilization buffer. Secondary antibodies (anti-goat-Alexa647 1:500 (Jackson Immunolabs), anti-rabbit-DyLight488 1:1,000 (Jackson Immunolabs), anti-mouse-DyLight549 1:1,000 (Jackson Immunolabs) were diluted in blocking buffer and applied for 1 hour at RT and 150 rpm in the dark. In the last 10 minutes, DAPI (1:10 000) was added for nuclear counterstaining. Cells were washed three times for 15 minutes with PBS. All centrifugation steps within the staining protocol were carried out at 900 rpm for 3 minutes at 4°C. After staining, cells were transferred to glasses coated with 0.3% (w/v) gelatin-deionized water for microscopically imaging using Quorum Spinning Disc Confocal 2 (Olympus) equipped with a Hamamatsu C9100-13 back-thinned EM-CCD camera (Hammamatsu).

Cardiomyocyte preparation and culturing

Hearts from auxilin knockout or wild-type neonatal mice were isolated and incubated in HBSS buffer supplemented with 5 mM BDM and 1 mg/ml collagenase type 2 overnight at 4°C with gentle shaking. Hearts were then transferred to mincing buffer (HBSS supplemented with 10 mM taurine, 10 mM BDM, 1 mg/ml BSA and 10 mg/ml collagenase type 2) and gently stirred for 7 minutes at 37°C in presence of a magnetic bar. Eluted cells were collected and filtered using a 100 µm strainer. The elution process was performed three times. Obtained cells were then washed in HBSS and spun down for 5 minutes at 4°C at 150 rcf (Sigma 3-18K centrifuge, rotor 11180, swing-out). Primary cardiomyocytes were plated at a density of $2.5x10^5$ cells/ml on 18 mm (time lapse recordings), $1.5x10^4$ cells/ml on 12 mm (Immunostaining) glasses coated with fibronectin supplemented with 0.02% gelatine solution and cultured over night or 48h at 37°C, 5% CO_2 in Claycomb medium supplemented with 10% FBS, 0.1 mM Norepinephrine, 2 mM L-glutamine and 100 µg/mL Penicillin/Streptomycin.

Human differentiated cardiomyocytes (iCell Cardiomyocytes[2], Cellular Dynamics International, Madison, WI, US) were cultured and harvested according to the manufacturer´s protocol.

Immunofluorescence staining of mouse primary cardiomyocytes

After preparation and culturing overnight, glasses with primary cardiomyocytes were washed twice in pre-warmed PBS and cells were fixed in 2% PFA/PBS for 10 minutes at RT. Quenching was carried out in 10 mM glycine/PBS for 10 minutes at RT followed by permeabilization of the cells in 0.1% (v/v) Triton for 10 minutes at RT. Blocking was performed with 5% BSA/PBS for 15 minutes at RT followed by primary antibody staining in 2.5% BSA/PBS for 1h at RT in a wet-chamber rabbit anti-auxilin (Sigma, HPA031182) 1:200, mouse anti-clathrin (Thermo Scientific, MA1-065), dilution 1:1200. Secondary antibody incubation was performed in 2.5% BSA/PBS for 20 minutes at RT in the dark (anti-mouse-Alexa546, anti-rabbit-Alexa488, (Thermo Fisher, Molecular Probes, US), dilutions 1:400). Nuclear staining with DAPI 1:20,000, was added to one of the secondary antibody staining solutions. One to three washing steps were performed in PBS or 2.5% BSA/PBS after each of the treatment steps. Glasses were washed in ddH_2O prior to mounting using Fluoromount G (Southern Biotechnology) and thereafter stored at 4°C in the dark.

Time lapse Ca^{2+} recordings

Cardiomyocytes were loaded with the Ca^{2+}-fluorescence indicator Fluo-4 AM (10 µM) (ref F14201, Molecular Probes, Life Technologies, Stockholm, Sweden) dissolved in DMSO (Invitrogen, UK), 0.2‰ pluronic acid (F-127, Life Technologies, Stockholm, Sweden) in 500 µl Claycomb supplemented culture medium without norepinephrine for 30 minutes at 37°C and 5% CO_2. Subsequently, de-esterification was performed in culture medium for 10 minutes (37˚C, 5% CO_2). Cover slips (18 mm) were mounted in a chamber and cytosolic Ca^{2+} measurements were carried out in complete medium supplemented with norepinephrine (final concentration 10 µM) at 37°C using a ZeissAxio Examiner D1. AX10 microscope (Zeiss 20x, water immersion objective, N.A. 1.0) equipped with a photometrics eVolve EMCCD-camera at a 0.1-2.0 s interval and filter set 38HE (Zeiss). Cardiomyocytes were perfused with complete medium (2.5 ml/min) using a peristaltic pump and temperature was controlled using a Chamlide Inline Heater (IL-H-10, Life Cell Instruments, Seoul, Korea) and Chamlide AC-PU perfusion chamber. Time-lapse calcium imaging time traces were normalized through $\Delta F/F_0$, where $\Delta F=F_1-F_0$. F_1 is the specific fluorescence intensity at a specific time point, and F_0 is the average intensity of 10 s before and after F_1.

Flow cytometry staining and analysis

Primary cardiocytes from mouse neonatal pups were prepared as described under primary cardiomyocyte preparation and culturing. For staining 0.1 mM EGTA was added to the mincing buffer. Obtained cells were stained with live/dead fixable violet dead stain 1:1,100 (Life Technologies, Sweden) for 10 minutes at RT. Cells were then pelleted and washed in HBSS supplemented with 0.1mM EGTA and 2% BSA. FcR blockade (anti-CD32/16 (eBioscience, US),

Meisgen S, *et al. Ann Rheum Dis* 2022;0:1–11. doi: 10.1136/annrheumdis-2021-221714

anti-CD64 (R&D Systems, UK) 1:500 and anti-CD89 1:200 (Santa Cruz, US)) was performed for 10 minutes at 4°C and gentle shaking. Cells were resuspended in 2% BSA/HBSS staining buffer containing anti-$Ca_v1.3$ primary antibody, 1:900 (Alomone Labs, Israel), and stained for 30 minutes at 4°C with gentle shaking. After washing, cells were stained with Alexa633 anti-rabbit 1:10,000 (Life Technologies, Sweden) and directly labelled anti-Sirpa-PE, 1:100 (BD Pharmingen, Europe) for 30 minutes at 4°C with gentle shaking. Cells were washed and transferred to HBSS buffer for flow cytometry analysis. Cardiac cell surface molecule expression was analyzed using a Gallios Flow Cytometer (Beckman Coulter, Sweden), and the data was analyzed with the FlowJo software (version 7.6.4, Ashland, US).

Doppler recordings

Pregnant mice were anesthetized with isoflurane (5% induction, 2% maintenance) and ultrasound examinations of the unborn mouse fetuses were performed with a Siemens S2000 ultrasound machine (Siemens Medical Solutions), equipped with a linear 18L6 HD transducer. Guided by color Doppler, pulsed Doppler recordings were obtained with a sample volume encompassing the whole heart in an angle showing inflow through the atrioventricular valves in a different direction from the outflow in the great arteries. Analysis and measurements on digitally stored Doppler tracings were made offline using a Siemens syngo US Workplace. Normal heart rate was defined as the 95% CI of that observed in wild-type fetal mice (100-225 bpm). The inflow a-wave, caused by atrial contraction, was used as marker of atrial activation and the outflow wave as marker of ventricular activation. Atrioventricular (AV)-time intervals used as a surrogate for the PR interval on the ECG were measured from the peak of the a-wave to the start of outflow profile. The isovolumetric contraction time (ICT) was measured from the end of AV inflow to the start of the outflow profile and the isovolumetric relaxation time from the end of the outflow profile to the beginning of ventricular filling. Measurements were made on three consecutive profiles and averaged.

The case presented in figure 7 was examined using the same ultrasound system with a 6C2 transducer. Moving 2D images, M-mode and pulsed Doppler recordings from the mitral valve and aortic outflow were used to diagnose cardiac rhythm and function.

Programs and statistical analysis

GWAS data was analyzed in the PLINK program (http://pngu.mgh.harvard.edu/~purcell/plink/). The R program (version 2.14.2) was used for eQTL analysis (lm package), probability and cardiac expression value plotting. All data processing time lapse $[Ca^{2+}]_i$ transients were performed with Image J 1.48 (Image J NIH, Bethesda, USA) and MatLab data system (Mat Works inc). Correlation analysis was performed with MatLab data system according to previous reports.[11, 12] This identifies intercell-synchronized Ca^{2+} peaks, visualizing cells that are connected to each other. Utilizing the MatLab BGL-library, network properties such as connectivity, mean shortest path-length and clustering coefficient were calculated to evaluate the organization of cardiac cell activity. Statistica and SigmaPlot were used to analyze the Doppler data and Graphpad Prism 5 was used for all other statistical tests. Statistical tests used for the individual experiments are stated in the respective figure legends. Schematic illustrations are from Servier Medical Art.

REFERENCES

1. A. Ambrosi *et al.*, Development of heart block in children of SSA/SSB-autoantibody-positive women is associated with maternal age and displays a season-of-birth pattern. *Annals of the rheumatic diseases* **71**, 334-340 (2012).
2. S. Salomonsson *et al.*, A population-based investigation of the autoantibody profile in mothers of children with atrioventricular block. *Scandinavian journal of immunology* **74**, 511-517 (2011).
3. C. International Multiple Sclerosis Genetics *et al.*, Genetic risk and a primary role for cell-mediated immune mechanisms in multiple sclerosis. *Nature* **476**, 214-219 (2011).
4. C. Coronary Artery Disease Genetics, A genome-wide association study in Europeans and South Asians identifies five new loci for coronary artery disease. *Nature genetics* **43**, 339-344 (2011).
5. A. L. Price *et al.*, Principal components analysis corrects for stratification in genome-wide association studies. *Nature genetics* **38**, 904-909 (2006).
6. L. Folkersen *et al.*, Association of genetic risk variants with expression of proximal genes identifies novel susceptibility genes for cardiovascular disease. *Circulation. Cardiovascular genetics* **3**, 365-373 (2010).

7. B. M. Bolstad, R. A. Irizarry, M. Astrand, T. P. Speed, A comparison of normalization methods for high density oligonucleotide array data based on variance and bias. *Bioinformatics* **19**, 185-193 (2003).
8. A. Dobin *et al.*, STAR: ultrafast universal RNA-seq aligner. *Bioinformatics* **29**, 15-21 (2013).
9. D. Ramskold, E. T. Wang, C. B. Burge, R. Sandberg, An abundance of ubiquitously expressed genes revealed by tissue transcriptome sequence data. *PLoS computational biology* **5**, e1000598 (2009).
10. Y. I. Yim *et al.*, Endocytosis and clathrin-uncoating defects at synapses of auxilin knockout mice. *Proceedings of the National Academy of Sciences of the United States of America* **107**, 4412-4417 (2010).
11. E. Smedler, S. Malmersjo, P. Uhlen, Network analysis of time-lapse microscopy recordings. *Frontiers in neural circuits* **8**, 111 (2014).
12. E. Smedler, P. Uhlen, Frequency decoding of calcium oscillations. *Biochimica et biophysica acta* **1840**, 964-969 (2014).

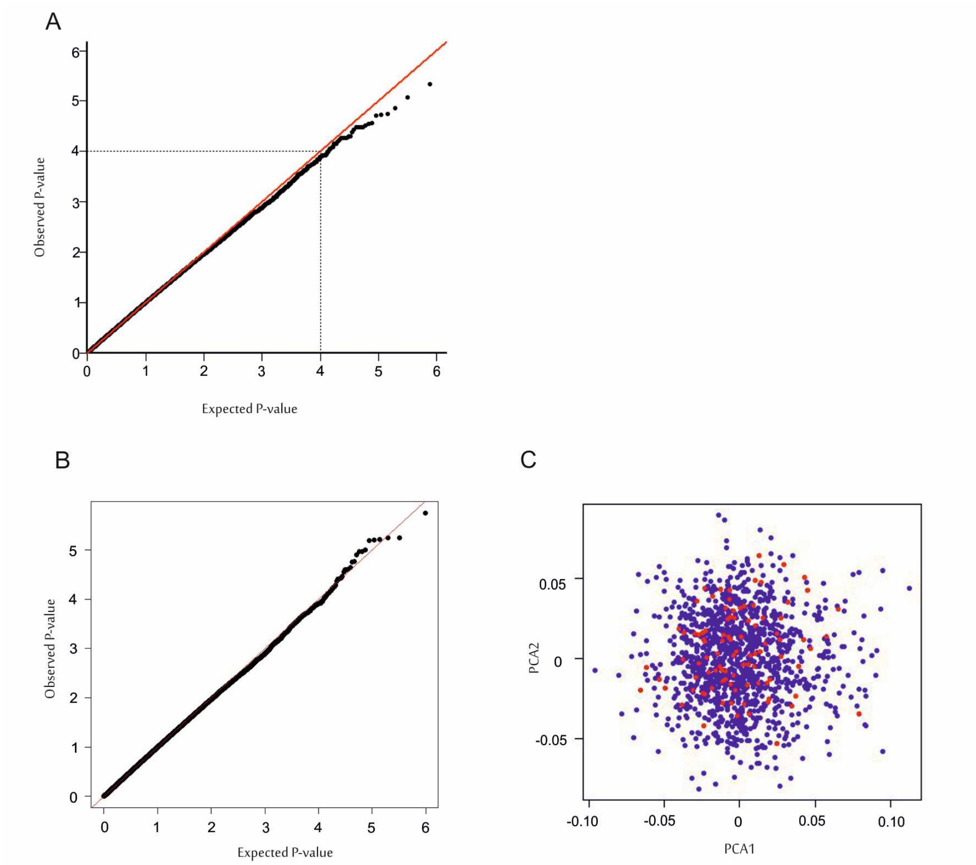

Supplemental Figure S1. Probability distributions and principal component analysis.

(A) Quantile-Quantile (Q-Q) plot for observed versus expected SNP associations in the CHB family analysis. Plot shows genome-wide associations (DFAM analysis) with CHB. The observed association significances are plotted against the expected association significance for included SNPs. The genomic control inflation factor was λ=1.01. Dashed lines indicate the cut-off for significances at $P < 10^{-4}$. (B) Q-Q-plot shows observed versus expected genome-wide SNP associations with CHB in the case-control analysis (logistic regression analysis after correction with one PCA). Plot excludes the extended MHC region chromosome 6:25-33Mb. The genomic inflation factor was λ=1.006 (A-B) Scales –log10. (C) Principal component analysis (PCA) plot of PCA2 versus PCA1 distribution among cases (red) and controls (blue).

Meisgen S, *et al. Ann Rheum Dis* 2022;0:1–11. doi: 10.1136/annrheumdis-2021-221714

A

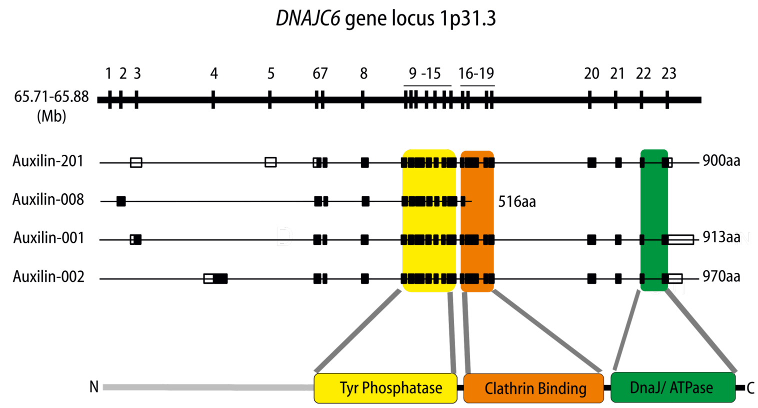

B

PCR amplicon	exon-exon boundary	forward primer	reverse primer	amplicon length
Auxilin-201	5-6	5' GAG TGG AAG GAG TCT GAA GAG AGG	5' CTA GAA GAT GTG TCT TTG AGG GTG	183
Auxilin-008	2-6	5' GAT GGG CGC CAC TGA GAA GG	5' GGT TAC TAA AGA GCC TCC CTG CAC	198
Auxilin-001	3-6	5' GAG GGA GGA AGC AGA GAA TGA AAG	5' GGT TAC TAA AGA GCC TCC CTG CAC	122
Auxilin-002	4-6	5' GGC GGC AAG CAG AGA GTG AAC G	5' GGT TAC TAA AGA GCC TCC CTG CAC	175
$Auxilin_{global}$	11-12	5' ACA GAG GAA TGG ATG TCG CCC T	5' AGC CGG CTC CCA ATG GTT GAC	195
ß2-microglobulin	1-4	5' TGC TCG CGC TAC TCT CTC TTT	5' TGT CGG ATG GAT GAA ACC CAG A	138

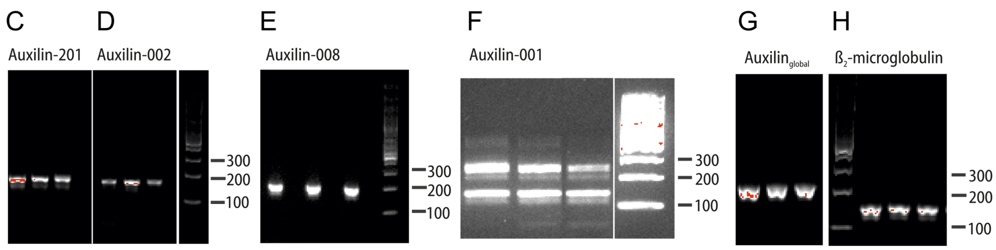

Supplemental Figure S2. PCR primer design for auxilin protein transcript variant expression analysis in cardiac tissue.

(A) *DNAJC6* gene locus (1p31.1) at 65.77-65.88 Mb including protein transcript variants and conserved protein domains. Red arrows indicate approximate location of forward and reverse primer annealing for amplification of each transcript variant. (B) Summary of qPCR primer design. The exon-exon boundary column lists exon junctions amplified according to genomic exon counting. Sequences for forward and reverse primers and PCR amplicon length are listed for each transcript variant. No primer design for unique amplification of auxilin-001 was possible. (C-H) PCR product size confirmation after amplification with the indicated primer pair on a 2% TBE agarose gel. GeneRulerTM DNA 100 bp ladder was used to determine PCR amplicon size. (C) Auxilin-201. (D) Auxilin-002. (E) Auxilin-008. (f) Auxilin-001. (G) $\text{Auxilin}_{\text{global}}$. (H) β2-microglobulin.

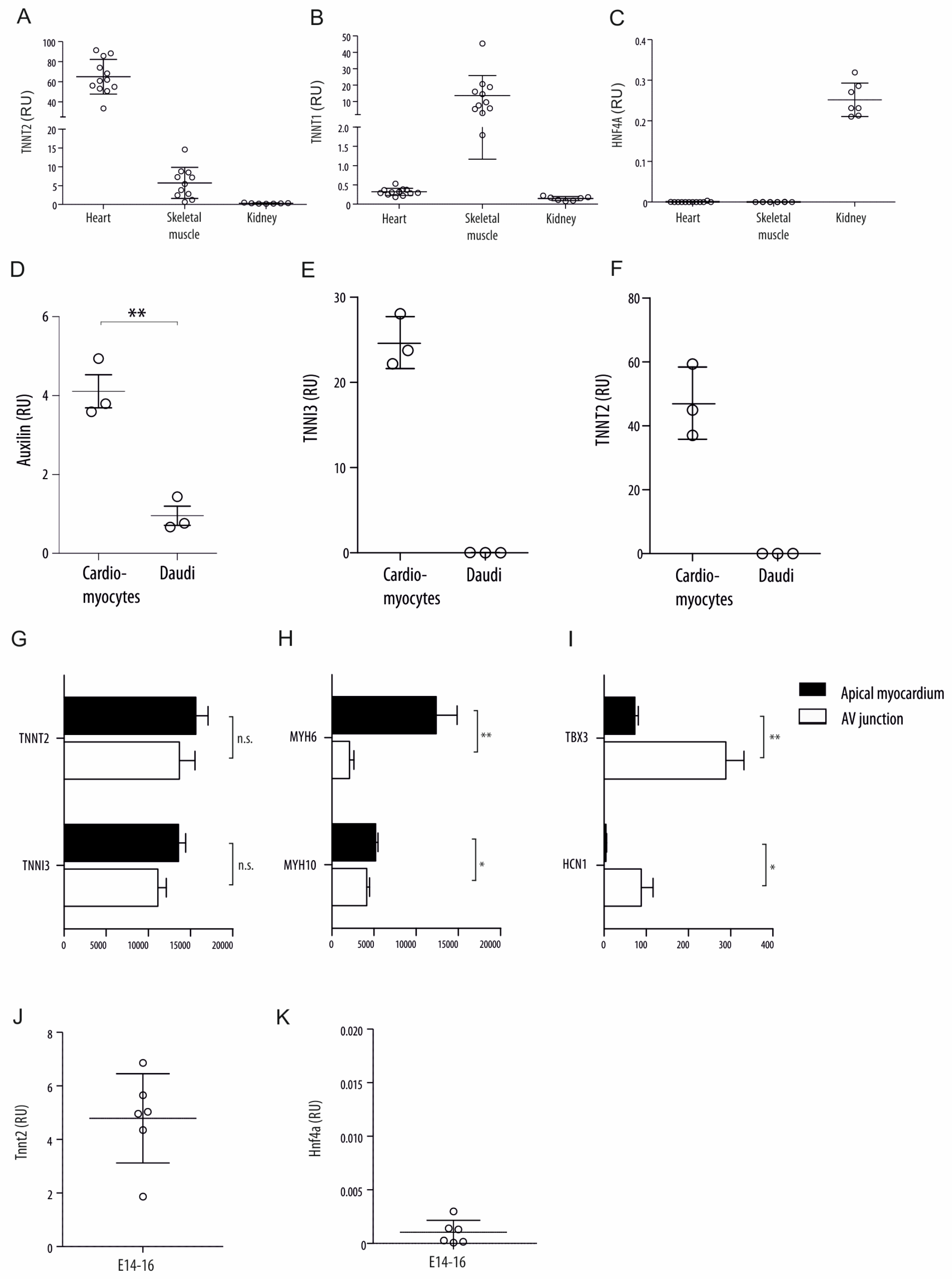
A
TNNT2 (RU)
Heart
Skeletal muscle
Kidney
B
TNNT1 (RU)
Heart
Skeletal muscle
Kidney
C
HNF4A (RU)
Heart
Skeletal muscle
Kidney
D
**
Auxilin (RU)
Cardio-myocytes
Daudi
E
TNNI3 (RU)
Cardio-myocytes
Daudi
F
TNNT2 (RU)
Cardio-myocytes
Daudi
G
TNNT2
TNNI3
n.s.
n.s.
H
MYH6
MYH10
**
*
I
TBX3
HCN1
**
*
Apical myocardium
AV junction
J
Tnnt2 (RU)
E14-16
K
Hnf4a (RU)
E14-16

Supplemental Figure S3. Confirmation of fetal and embryonic mouse tissue identity, cardiomyocyte auxilin RNA expression and cell-type identity.

(A-C) Identity of fetal tissue (week 10-12 of gestation) was confirmed by qPCR of tissue-specific genes (expression level relative to β2-microglobulin). (A) Cardiac tissue identity was verified by high *TNNT2* expression (>30 AU) in n=12 samples. Samples with low expression were excluded from further analysis. *TNNT2* expression was used as a tissue negative marker for skeletal muscle and kidney samples. (B) Skeletal muscle identity was verified via *TNNT1* expression (>1.5 AU) and n=11 samples were included. *TNNT1* expression was not observed in cardiac or renal tissue. (C) Kidney tissue identity was tested by *HNF4A* expression (>0.2 AU) analysis and n=7 samples were included. The renal tissue marker was not expressed in the other tested tissues. Bars represent mean ± s.d. (D) Auxilin RNA expression in human cardiomyocytes from induced iPS cells compared to Daudi cells. (D-F) Identity of cardiac tissue was confirmed by qPCR of tissue-specific genes (expression level relative to β2-microglobulin). Cardiac tissue identity was verified by high *TNNI3* (E) and *TNNT2* (F) expression (>20 RU) in iCell cardiomyocyte cultures (n=3). Daudi cells (n=3) were used as a negative control for tissue specific gene expression. Bars represent mean ± s.e.m. (G-I) Identity of apical myocardial and AV junctional tissue after microdissection of human fetal hearts (n=6; gestational age 20-22 weeks) was confirmed by gene expression analysis. Expression levels are arbitrary units relative to all genes expressed on the Affymetrix Human U133 plus 2 Array. (G) Cardiac tissue identity was verified by high *TNNT2* and *TNNI3* expression among all samples taken. (H) Apical myocardial identity was confirmed by MYH6 and MHY10 expression and (I) AV junctional identity by *TBX3* and *HCN1* specific gene expression. (J, K) Quantitative PCR for cardiac cell-type identity in embryonic wildtype mice relative to Taf8 expression. (J) Cardiac tissue specificity was verified by Tnnt2 expression (>0.5 AU) in samples from mouse fetuses (E14-16, n=6). (K) Hnf4a (kidney marker) expression levels were used as tissue negative markers. Bars represent mean ± s.d. Bars represent mean ± s.e.m. * $p < 0.05$, ** $p < 0.01$

Meisgen S, *et al. Ann Rheum Dis* 2022;0:1–11. doi: 10.1136/annrheumdis-2021-221714

Supplemental Table S1. Clinical characteristics of the mothers and their children with congenital heart block.

Maternal age at blood sampling mean (95% CI)	53.8 (50.8-56.8)
Maternal diagnosis[1] n (%)	(n=88)
pSS	14 (16%)
SLE	12 (14%)
SLE with sSS	18 (20%)
RA	1 (1%)
RA with sSS	1 (1%)
No rheumatic diagnosis	39 (44%)
Not available[2]	2 (2%)
Autoantibodies[3] n (%)	(n=80)
anti-Ro52	77 (96%)
anti-Ro60	49 (61%)
anti-La	46 (58%)
anti-Histone	6 (8%)
anti-SmB	1 (1%)
anti-SmD	3 (4%)
anti-RNP	2 (2%)
anti-Cenp-B	2 (2%)
anti-Ribosomal P	1 (1%)
Diagnosis in the children[4]	(n=92)[5]
AVB II-III	92
AVB I	0

[1]Clinical diagnosis registered at the time of sampling of the family.
[2]Deceased/lost to follow-up
[3]Sera available from 80 mothers
[4]Highest degree of AVB observed
[5]Four mothers each gave birth to two children with AVB II-III.

Supplemental Table S2. Genetic regions associated with CHB at PDFAM1≤ 1x10-4.[1]

Chr	SNP marker	Position	RA	$RAF_{[founders]}$	P-value	Trans[%]	OR(CI)	Gene	Region
1	rs1570868	65603196	A	0.461	3.27E-05	75.00	3.00 (1.73-5.19)	*DNAJC6*	intronic
1	rs6588138	65610954	A	0.471	7.06E-05	75.38	3.06 (1.74-5.38)	*DNAJC6*	intronic
1	rs3818513	65646625	A	0.441	7.06E-05	25.00	0.33 (0.18-0.58)	*DNAJC6*	intronic
1	rs7552323	167369947	A	0.449	8.22E-05	71.05	2.45 (1.49-4.03)	*NME7*	intronic
2	rs1477511	220330082	C	0.144	2.78E-05	86.67	6.50 (2.26-18.62)	*SLC4A3*	intergenic
3	rs12633887	15564595	A	0.274	5.69E-05	77.97	3.53 (1.91-6.54)	*PHYH2*	intergenic
3	rs1993331	16047351	G	0.240	5.47E-05	78.26	3.60 (1.78-7.25)	*GALNTL2*	intergenic
3	rs2730367	16048270	G	0.240	5.47E-05	78.26	3.60 (1.78-7.25)	*GALNTL2*	intergenic
3	rs2730335	16052851	A	0.240	5.47E-05	78.26	3.60 (1.78-7.25)	*GALNTL2*	intergenic
7	rs11983987	75495786	G	0.174	3.66E-05	84.62	5.50 (2.30-13.13)	*STYXL1*	intronic
7	rs1639609	75521517	G	0.341	3.36E-05	75.41	3.06 (1.71-5.49)	*MDH2*	intronic
7	rs4732595	75593075	G	0.341	9.57E-05	73.33	2.75 (1.55-4.87)	*MDH2*	intergenic
7	rs10085567	75572142	C	0.341	3.36E-05	75.41	3.06 (1.71-5.49)	*MDH2*	intergenic
7	rs6953665	75606985	A	0.329	5.01E-05	75.00	3.00 (1.67-5.38)	*MDH2*	intergenic
9	rs4540481	29980455	A	0.368	8.32E-05	72.58	2.64 (1.51-4.62)	*LRRN6C*	intergenic
9	rs12552164	30007230	A	0.380	7.18E-05	72.31	2.61 (1.51-4.49)	*LRRN6C*	intergenic
9	rs12375503	30028860	A	0.387	1.36E-05	75.00	3.00 (1.70-5.28)	*LRRN6C*	intergenic
9	rs4745225	75030376	C	0.203	5.18E-05	18.42	0.22 (0.09-0.51)	*ANXA1*	intergenic
12	rs2030130	24165338	G	0.169	8.50E-06	84.38	5.40 (2.08-14.02)	*SOX5*	intronic
12	rs10878353	64668799	G	0.201	8.93E-05	79.55	3.88 (1.86-8.09)	*HMGA2*	intergenic
12	rs10878354	64671152	A	0.201	8.93E-05	79.55	3.88 (1.86-8.09)	*HMGA2*	intergenic
12	rs719450	119438416	A	0.160	6.25E-05	79.41	3.85 (1.68-8.85)	*COQ5*	intronic
15	rs17521464	94384822	G	0.169	6.02E-05	80.00	4.00 (1.84-8.68)	*NR2F2*	intergenic
18	rs981738	63980419	C	0.157	2.88E-05	83.78	5.16 (2.15-12.38)	*TXNDC10*	intergenic
18	rs641672	63980432	G	0.158	1.81E-05	84.21	5.33 (2.23-12.75)	*TXNDC10*	intergenic
20	rs2148218	54324150	G	0.246	5.50E-05	22.92	0.29 (0.15-0.58)	*C20orf108*	intergenic

20	rs6024799	54338231	C	0.287	1.87E-05	19.61	0.24 (0.12-0.48)	*C20orf108*	intergenic
20	rs988166	54354265	G	0.246	8.38E-05	23.40	0.30 (0.15-0.60)	*C20orf108*	intergenic
20	rs8118732	54356605	G	0.190	1.92E-05	16.22	0.19 (0.08-0.46)	*C20orf108*	intergenic
20	rs6099095	54357169	A	0.194	3.05E-05	16.67	0.20 (0.08-0.48)	*C20orf108*	intergenic
20	rs6024830	54371614	A	0.269	5.50E-05	22.92	0.29 (0.15-0.58)	*C20orf108*	intronic
21	rs1394369	23690630	G	0.364	4.67E-06	20.31	0.25 (0.13-0.46)	*C21orf74*	intergenic

[1]The analysis of association was performed using the family-based association for disease trait (DFAM) analysis. CHB cases (n=92), first degree relatives (n=256). Associations with $P \leq 1x10^{-4}$ are included.

Chr, chromosome; RA, risk allele; RAF, risk allele frequency; Trans, parental transmission frequency to index cases; OR, odds ratio; CI, 95% confidence interval.

Supplemental Table S3. Validation analysis of CHB-associated SNPs at PDFAM≤ 1x10-4 using a case-control design.[1]

Chr	SNP marker	Position	RA	$RAF_{cases/\ controls}$	P-value	OR(CI)	Gene	Region
1	rs1570868	65603196	A	0.588/ 0.421	6.22E-06	2.01 (1.50-2.81)	*DNAJC6*	intronic
1	rs6588138	65610954	A	0.537/ 0.416	1.36E-03	1.66 (1.22-2.27)	*DNAJC6*	intronic
1	rs3818513	65646625	A	0.375/ 0.481	5.84E-03	0.64 (0.47-0.88)	*DNAJC6*	intronic
1	rs7552323	167369947	A	0.557/ 0.408	2.20E-04	1.82 (1.33-2.49)	*NME7*	intronic
2	rs1477511	220330082	C	0.182/ 0.105	2.73E-03	1.92 (1.25-2.94)	*SLC4A3*	intergenic
3	rs12633887	15564595	A	0.365/ 0.298	1.51E-01	1.27 (0.92-1.75)	*PHYH2*	intergenic
3	rs1993331	16047351	G	0.302/ 0.175	3.10E-04	1.86 (1.33-2.61)	*GALNTL2*	intergenic
3	rs2730367	16048270	G	0.304/ 0.174	2.20E-04	1.90 (1.35-2.67)	*GALNTL2*	intergenic
3	rs2730335	16052851	A	0.297/ 0.173	5.20E-04	1.82 (1.30-2.56)	*GALNTL2*	intergenic
7	rs11983987	75495786	G	0.255/ 0.206	1.17E-01	1.33 (0.93-1.90)	*STYXL1*	intronic
7	rs1639609	75521517	G	0.417/ 0.324	4.61E-02	1.40 (1.01-1.94)	*MDH2*	intronic
7	rs10085567	75572142	C	0.417/ 0.323	4.50E-02	1.40 (1.01-1.95)	*MDH2*	intergenic
7	rs4732595	75593075	G	0.417/ 0.323	4.40E-02	1.40 (1.01-1.94)	*MDH2*	intergenic
7	rs6953665	75606985	A	0.412/ 0.321	6.04E-02	1.37 (0.99-1.90)	*MDH2*	intergenic
9	rs4540481	29980455	A	0.438/ 0.328	1.13E-02	1.50 (1.10-2.06)	*LRRN6C*	intergenic
9	rs12552164	30007230	A	0.443/ 0.336	1.39E-02	1.49 (1.08-2.04)	*LRRN6C*	intergenic
9	rs12375503	30028860	A	0.458/ 0.341	5.16E-03	1.56 (1.14-2.14)	*LRRN6C*	intergenic
9	rs4745225	75030376	C	0.147/ 0.198	1.06E-01	0.70 (0.46-1.08)	*ANXA1*	intergenic
12	rs2030130	24165338	G	0.243/ 0.149	1.75E-03	1.63 (1.13-2.35)	*SOX5*	intronic
12	rs10878353	64668799	G	0.276/ 0.213	3.72E-02	1.47 (1.02-2.11)	*HMGA2*	intergenic
12	rs10878354	64671152	A	0.276/ 0.219	5.34E-02	1.43 (1.00-2.06)	*HMGA2*	intergenic
12	rs719450	119438416	A	0.214/ 0.139	6.81E-03	1.76 (1.17-2.65)	*COQ5*	intronic
15	rs17521464	94384822	G	0.229/ 0.184	2.84E-01	1.22 (0.85-1.76)	*NR2F2*	intergenic
18	rs981738	63980419	C	0.211/ 0.207	9.34E-01	1.02 (0.70-1.48)	*TXNDC10*	intergenic
18	rs641672	63980432	G	0.214/ 0.190	8.95E-01	1.03 (0.70-1.50)	*TXNDC10*	intergenic
20	rs2148218	54324150	G	0.177/ 0.253	3.52E-02	0.65 (0.43-0.97)	*C20orf108*	intergenic

20	rs6024799	54338231	C	0.186/ 0.280	1.93E-02	0.63 (0.42-0.93)	*C20orf108*	intergenic
20	rs988166	54354265	G	0.172/ 0.252	4.43E-02	0.65 (0.43-0.99)	*C20orf108*	intergenic
20	rs8118732	54356605	G	0.104/ 0.204	6.14E-03	0.50 (0.30-0.82)	*C20orf108*	intergenic
20	rs6099095	54357169	A	0.104/ 0.204	6.14E-03	0.50 (0.30-0.82)	*C20orf108*	intergenic
20	rs6024830	54371614	A	0.177/ 0.276	1.60E-02	0.61 (0.41-0.91)	*C20orf108*	intronic
21	rs1394369	23690630	G	0.266/ 0.352	1.77E-02	0.66 (0.46-0.93)	*C21orf74*	intergenic

[1]Logistic regression analysis after PCA correction (one significant PCA vector) of SNPs associated with CHB ($P \leq 1x10^{-4}$) in the DFAM analysis between cases (n=89) and controls (n=1112). λ=1.006**.**

Chr, chromosome; RA, risk allele; RAF, risk allele frequency; Trans, parental transmission frequency to index cases; OR, odds ratio; CI, 95% confidence interval.

Supplemental Table S4. Cardiac abnormalities in auxilin-deficient mouse fetuses.[1]

	Auxilin$^{+/+}$ (n=147)	Auxilin$^{+/-}$ (n=89)	Auxilin$^{-/-}$ (n=131)	*P*-values[2]
Gestational age (days)	14.6±2.2	14.7±2.0	14.2±2.1	*0.15 (0.24)*
Intrauterine death	2	1	1	
Heart rate (bpm)	162±32	160±30	160±42	*0.89 (0.89)*
Mechanical time intervals				
AV-time (ms)	69.8±13.1	72.7±15.0	78.9±22.4	***0.014 (0.010)***
ICT (ms)	32.5±9.9	36.3±12.4	41.1±14.2	***<0.001 (<0.001)***
IRT (ms)	54.2±9.4	52.6±9.6	50.1±12.4	*0.29 (0.35)*
ET (ms)	136.7±29.6	133.5±28.5	137.5±31.9	*0.72 (0.98)*
Abnormal heart rhythm				
Atrial pause	2			
Atrial arrest with VES	1	2		
SVES (> 1:5)	1	2	16	
VES (> 1:5)	1	4		
AV-block II (Mobitz II)		2		
Abnormal heart rate (HR) and rhythm				
Tachycardia (HR>225 bpm)	6	1	9	
Tachycardia with SVES			1	
Bradycardia (HR<100 bpm)	2	3	2	
Bradycardia with VES		2	3	
Bradycardia with atrial pause			1	
Ectopic beats with normal heart rate	1/137 (1%)	4/82 (5%)	22/114 (19%)	***<0.001 (<0.001)***
Ectopic beats	1/145 (1%)	6/88 (7%)	26/130 (20%)	***<0.001 (<0.001)***
Abnormal rate or rhythm	11/145 (9%)	12/88 (15%)	38/130 (30%)	***<0.001 (<0.001)***

[1]Doppler echocardiographic measurements in fetuses *in utero*. Values represent number of affected mouse fetuses or mean ± 1 SD. AV, atrioventricular; AV-time, mechanical estimate of the PR-interval on ECG; ICT, isovolumetric contraction time; IRT, isovolumetric relaxation time; ET, ejection time; SVES, supraventricular ectopic beats, VES, ventricular ectopic beats. [2]*P*-values denote statistics comparing all three groups of genotypes (One-way ANOVA (Tukey HSD), Kruskal-Wallis (Dunn´s post hoc), Chi square 2x3 contingency table). *P*-values comparing auxilin$^{+/+}$ versus auxilin$^{-/-}$ are given within parentheses.

SUPPLEMENTAL MOVIE LEGENDS

Supplemental Movie S1. Parallel display of $[Ca^{2+}]_i$ oscillations in cultured primary neonatal auxilin wild-type and knockout cardiomyocytes. Time-lapse imaging showing $[Ca^{2+}]_i$ oscillations and connectivity in primary neonatal cardiomyocytes from auxilin wild-type ($Aux^{+/+}$, left) and knockout ($Aux^{-/-}$, right) mice. Cells from littermates were pooled and cultured on collagen at a density of $2.5x10^5$ cells/mL for 48h before visualization by Fluo4-AM. 1 second corresponds to 15 seconds real time (30 frames per second).

Supplemental Movie S2. Parallel phase-contrast display of cultured primary neonatal auxilin wild-type and knockout cardiomyocytes. Phase-contrast time-lapse imaging sequence showing connectivity and physical contractions in primary neonatal cardiomyocytes from auxilin wild-type ($Aux^{+/+}$, left) and knockout ($Aux^{-/-}$, right) mice. Cells from littermates were pooled and cultured on collagen at a density of $2.5x10^5$ cells/mL for 48h before time-lapse imaging. 1 second corresponds to 15 seconds real time (30 frames per second).

Supplemental Movies S3 and S4. Doppler echocardiographic recordings of mouse fetuses *in utero*.

Supplemental Movie S3. 2D moving image of a pregnant mouse showing three of her fetuses with their placentas *in utero*. The heart activity is clearly seen.

Supplemental Movie S4. 2D moving image with color Doppler showing three mouse fetuses *in utero*. Note the typical flow pattern in the heart with inflows through the AV-valves and outflows in the great arteries in opposite directions. Flow towards the transducer is coded red and flow from the transducer is coded blue.

Supplemental Movies S5 and S6. A case of junctional ectopic tachycardia progressing to CHB in a human fetus.

Supplemental Movie S5. 2D moving image corresponding to Figure 7l,m (gestation age 21 weeks). Transverse thoracic cut showing the heart in a 4 chamber view. The heart has a normal size and structure. Heart rhythm and rate are normal; however those are not generated in the atria but from an ectopic focus.

Supplemental Movie S6. 2D moving image of the same case as in Supplementary Movie S5, but 3 weeks later (gestational age 24 weeks), corresponding to Figure 7n,o. Transverse thoracic cut showing the heart in a 4 chamber view. The heart is dilated with patchy echogenic changes, diagnosed as cardiomyopathy and endocardial fibroelastosis. The rhythm is regular but slow at 46 beats per minute.